

(1954); I. Talmi, *ibid.* **126**, 1096 (1962).

⁵⁷D. D. Armstrong and A. G. Blair, *Phys. Rev.* **140**, B1226 (1965).

⁵⁸G. Brown, J. G. B. Haigh, and A. E. MacGregor, *Nucl. Phys.* **A97**, 353 (1967).

⁵⁹W. Fitz, J. Heger, R. Jahr, and R. Santo, *Z. Physik*

202, 109 (1967).

⁶⁰M. S. Freedman, F. Wagner, Jr., F. T. Porter, and H. H. Bolotin, *Phys. Rev.* **146**, 791 (1966).

⁶¹A. Bernstein, in *Advances in Nuclear Physics*, edited by M. Baranger and E. Vogt (Plenum Press, Inc., New York, to be published), Vol. III.

PHYSICAL REVIEW C

VOLUME 2, NUMBER 1

JULY 1970

Shell-Model Structure of $^{42-50}\text{Ca}^\dagger$

J. B. McGrory, B. H. Wildenthal,* and E. C. Halbert
Oak Ridge National Laboratory, Oak Ridge, Tennessee 37830

(Received 12 January 1970)

The low-lying states of the calcium isotopes ^{42}Ca through ^{50}Ca are discussed within the framework of the conventional shell model. An inert ^{40}Ca core is assumed. Calculations are made in several basis-vector spaces involving active $0f_{7/2}$, $1p_{3/2}$, $0f_{5/2}$, $1p_{1/2}$, and $0g_{9/2}$ neutron orbits. In one set of calculations, we use a "realistic" effective interaction derived for this mass region by Kuo and Brown. The shell-model results suggest that, in this effective interaction, the interactions of $f_{7/2}$ neutrons with $p_{3/2}$, $p_{1/2}$, and $f_{5/2}$ neutrons are too strong. In other calculations, with a modified Kuo-Brown interaction, we find the calculated spectra for the low-lying states of the calcium isotopes are in agreement with observed spectra, with several significant exceptions. The exceptions are that the second 0^+ and 2^+ states observed in ^{42}Ca , ^{44}Ca , and ^{46}Ca are not accounted for in the calculation. Calculated spectroscopic factors for $f_{7/2}$ transfers are in good agreement with experimental spectroscopic factors, and the observed centroids of the $p_{3/2}$ single-particle strengths are reasonably well reproduced. Our results also indicate that "core-excitation" effects are significant above about 2.5 MeV in ^{42}Ca through ^{48}Ca .

I. INTRODUCTION

The low-lying levels of the calcium isotopes have long been of interest to both experimental and theoretical physicists. Thirteen isotopes of calcium are known, six of which are stable. Using these six stable isotopes as targets, it is possible to study the level structure of all 13 isotopes with one- and two-nucleon pickup and stripping reactions. Thus it has been possible to accumulate a large amount of experimental information about these nuclei. The calcium isotopes comprise a convenient set of nuclei from a theoretical standpoint too. With the exception of the lightest two isotopes, ^{38}Ca and ^{39}Ca , it is useful to make the approximation that each calcium isotope has a doubly-magic $A=40$ core. In this approximation, all the active particles outside the $A=40$ core are neutrons. Then with some further simplifications (which we shall discuss), detailed shell-model treatments of the Ca isotopes become quite feasible. These further simplifications are suggested by the spectrum of single-particle states that seems to be appropriate for the calcium isotopes. The single-particle spectrum will be discussed in

more detail in Sec. II.

Many calculations of the level structures of the calcium isotopes have been reported previously. It is useful to describe briefly several such calculations, as a background to the investigation reported here. In the earliest systematic calculations of the calcium isotopes,¹⁻³ only pure $f_{7/2}$ -neutron configurations were included. The structure of the single-particle spectrum, as discussed below, suggests that this pure- $f_{7/2}$ model is a reasonable first-order approximation. In this approximation the effective Hamiltonian is completely specified by five parameters: the binding energy of the $f_{7/2}$ neutron to the ^{40}Ca core, and the four two-body matrix elements $\langle f_{7/2}^2 J | V | f_{7/2}^2 J \rangle$ with $J=0, 2, 4, \text{ and } 6$. (Here, and throughout this paper, V represents the two-body part of the effective Hamiltonian.) In the calculations of Refs. 1-3, these five parameters were taken directly from the experimentally observed spectra of ^{41}Ca and ^{42}Ca . These calculations satisfactorily reproduced the observed energies and spins of many of the low-lying states of the calcium isotopes. The levels which are accounted for by this pure- $f_{7/2}$ model will be referred to as $f_{7/2}$ states.

In a later calculation, reported by Raz and Soga,⁴ active $p_{3/2}$ neutrons were allowed, as well as active $f_{7/2}$ neutrons. The four isotopes ^{42}Ca through ^{45}Ca were treated. All possible configurations of particles distributed in the $f_{7/2}$ and $p_{3/2}$ orbits were included in the basis-vector space. The $f_{7/2}$ and $p_{3/2}$ single-particle energies were taken from observed states in ^{41}Ca ; and the two-body interaction was parametrized with seven strengths which were adjusted so as to give least-squares fits to several alternative sets of experimentally determined energy levels. (These several sets contained from 18 to 22 levels.) The results of this seven-parameter calculation indicated the importance of active $p_{3/2}$ neutrons in certain low-lying $\frac{3}{2}^-$ states of ^{43}Ca and ^{45}Ca . In another systematic calculation of the calcium isotopes, Engeland and Osnes⁵ included all pure- $f_{7/2}$ configurations, and all configurations in which only one neutron is excited from the $f_{7/2}$ orbit to the $p_{3/2}$ orbit. With this restriction, and with the assumption that the effective residual Hamiltonian contains only one-body and two-body terms, the Hamiltonian is defined by two single-particle energies and ten two-body matrix elements. Engeland and Osnes took the single-particle energies from the experimentally observed spectrum of ^{41}Ca , and then treated the ten two-body matrix elements as variable parameters in a least-squares fit to 20 experimental levels in ^{42}Ca to ^{47}Ca . In these Raz-Soga⁴ and Engeland-Osnes⁵ calculations, both of which included some configurations involving active $p_{3/2}$ neutrons, the quality of agreement with experiment was very similar. Neither calculation could account for the first excited 0^+ and second 2^+ state in ^{42}Ca and ^{44}Ca . From both calculations, it was concluded that these particular 0^+ and 2^+ states contained important contributions from configurations not included in the model vector spaces that were used.

In another calculation, reported by Federman and Talmi,⁶ all possible configurations of the form $(f_{7/2}^n)$, $(f_{7/2}^{n-1}p_{3/2})$, and $(f_{7/2}^{n-2}p_{3/2}^2)$ were included. In this space the effective model Hamiltonian is specified by 15 two-body matrix elements and two single-particle energies. The single-particle energies were again taken from the observed spectrum of ^{41}Ca . Two of the 15 two-body matrix elements were fixed at values determined in a previous calculation, and the remaining 13 were treated as adjustable parameters. Furthermore, the second 0^+ and 2^+ states in ^{42}Ca were assumed to contain significant admixtures of deformed states, and the effects of these deformed states on the spectrum of ^{42}Ca were introduced in a way that involved one more adjustable parameter. Thus there were 14 adjustable parameters in all. These

14 parameters were determined by a least-squares fit to 30 observed levels in the nine isotopes ^{42}Ca to ^{50}Ca . In this calculation, it was possible to account for the energies of these second 0^+ and 2^+ states in ^{44}Ca with $f_{7/2}$ and $p_{3/2}$ active neutrons only. This conclusion was in contradiction to the conclusions of Raz and Soga and of Engeland and Osnes.

In addition to the questions raised by these contradictory results, the recent accumulation of many new experimental data suggests that a more extensive calculation of the calcium isotopes could be useful. These new data include empirically determined spectroscopic factors both for single-neutron transfer reactions, and for two-neutron transfer reactions to states in the even calcium isotopes. In this paper we limit ourselves to discussing energy levels, ground-state binding energies, and spectroscopic factors for one-neutron transfer reactions. (We defer discussion of two-nucleon transfer, and of electromagnetic moments and transition rates, to a subsequent paper.) In the calculations to be discussed in this paper, we allow some active neutrons in each of the orbits in the f - p shell. In some calculations we also allow some active $g_{9/2}$ neutrons. The model vector spaces are described more exactly in the next section. We believe that we have included all those configurations involving f - p -shell particles outside an inert ^{40}Ca core which are significantly admixed into the low-lying states of the calcium isotopes. We use the effective residual interaction derived by Kuo and Brown⁷ from the Hamada-Johnston free nucleon-nucleon potential. Also, we investigate some variations of the Kuo-Brown interaction. One purpose of our calculations is to assess the quality of agreement obtainable in shell-model calculations which use the Kuo-Brown interaction. Our hope is that the results of this investigation lead to reasonable conclusions as to which of the experimentally observed calcium states can or cannot be accounted for by f - p -shell configurations. This hope is based, to some extent, on the success of similar calculations of the structure of light s - d -shell nuclei.⁸

In Sec. II we give details about the basis-vector spaces we have used, and the model Hamiltonians we have used. In Sec. III we discuss the energy levels and spectroscopic factors calculated for ^{42}Ca to ^{50}Ca from the Kuo-Brown interaction. In Sec. IV we discuss the analogous results obtained from a *modified* version of the Kuo-Brown interaction. (This modified version gives distinct improvement for certain selected levels.) In Sec. V we present results for ground-state binding energies. A brief summary of all the results is presented in Sec. VI.

II. BASIS-VECTOR SPACES AND MODEL HAMILTONIANS

The calculations we shall discuss are all made within the framework of the conventional shell model. We assume a truncated set of active single-particle orbits, and form multiparticle basis states by distributing neutrons in these active orbits. We then diagonalize a model Hamiltonian in the space of these basis states. The eigenvalues are identified as nuclear energy levels, and the eigenvectors as wave functions of nuclear states. All the calculations have been made with the help of the Oak Ridge-Rochester shell-model computer programs.⁹

We shall discuss calculations involving two alternative basis-vector spaces. For both spaces an inert ^{40}Ca core is assumed. For the first space, all the f - p -shell single-neutron orbits are active — i.e., the $f_{7/2}$, $p_{3/2}$, $p_{1/2}$, and $f_{5/2}$ orbits. For the second space, the $g_{9/2}$ neutron orbit is active as well as the f - p -shell orbits. For each isotope of mass A , we include all Pauli-allowed configurations of the form $(f_{7/2}^{n_1} p_{3/2}^{n_2})$, where $n_1 + n_2 = A - 40$. In addition, we include all Pauli-allowed configurations of the form $(f_{7/2}^{n_1} p_{3/2}^{n_2} j_1^{n_3} j_2^{n_4})$, where $n_1 + n_2 + n_3 + n_4 = A - 40$ and $n_3 + n_4 \leq 2$. In the first space, j_1 and j_2 can be either $p_{1/2}$ or $f_{5/2}$; and in the second space, j_1 and j_2 can be either $p_{1/2}$, $f_{5/2}$, or $g_{9/2}$. Thus for both spaces we restrict the number of neutrons distributed among the $p_{1/2}$, $f_{5/2}$, and $g_{9/2}$ orbits to two or fewer. This restriction is necessary for the heavier isotopes ($A \geq 46$), in order to limit the size of the matrices to manageable proportions. This truncation scheme is suggested by the experimentally observed ^{41}Ca spectrum (which we shall discuss soon).

We shall start by discussing calculations which use an effective interaction derived by Kuo and Brown⁷ for the f - p -shell region of the Periodic Table. This interaction was designed for use in the shell-model vector space spanned by all Pauli-allowed states of active particles distributed among the $f_{7/2}$, $p_{3/2}$, $p_{1/2}$, $f_{5/2}$, and $g_{9/2}$ orbits. This is not the space used in any of the calculations we shall discuss here, since in our calculations the number of particles distributed among the $p_{1/2}$, $f_{5/2}$, and $g_{9/2}$ orbits is always restricted to 0, 1, or 2. We justify our use of the Kuo-Brown interaction in this restricted vector space as follows. Suppose that we were interested in calculations in a vector space limited to neutron configurations of the form $(f_{7/2}^{n_1} p_{3/2}^{n_2})$. Suppose also that instead of using the published Kuo-Brown interaction, we followed the Kuo-Brown prescription to generate an effective interaction for this

$f_{7/2}$ - $p_{3/2}$ shell-model calculation. Then any effects due to the excitation of particles to the $p_{1/2}$, $f_{5/2}$, or $g_{9/2}$ orbits would be included only as second-order renormalizations of the $f_{7/2}$ - $p_{3/2}$ effective interaction. These second-order renormalizations would involve only one- and two-body excitations out of the $f_{7/2}$ - $p_{3/2}$ space. But in the shell-model calculations to be described in this paper, the $p_{1/2}$, $f_{5/2}$, and $g_{9/2}$ are treated more fully — for we explicitly include, in the first space, configurations with one- and two-particle excitations to the $p_{1/2}$ and $f_{5/2}$ orbits; and in the second space we include configurations with one- and two-particle excitations to the $p_{1/2}$, $f_{5/2}$, and $g_{9/2}$ orbits; i.e., the effects of these excitations on the states dominated by $(f_{7/2}^{n_1} p_{3/2}^{n_2})$ configurations are treated by diagonalization, rather than by second-order perturbation theory. Thus, insofar as states dominated by $(f_{7/2}^{n_1} p_{3/2}^{n_2})$ configurations are concerned, the calculations reported here represent an improvement over a calculation in which the explicit shell-model basis involves only $(f_{7/2} p_{3/2})$ configurations, while the effects of other f - p -shell configurations are introduced via second-order renormalization of the effective interaction. In fact, we have checked the effect of our vector-space limitation by comparison with results from some calculations using the vector space for which the Kuo-Brown interaction was designed. In particular, we calculated shell-model energy spectra for ^{43}Ca and ^{44}Ca using the Kuo-Brown interaction in the complete space of multiparticle states formed by distributing neutrons among the $f_{7/2}$, $p_{3/2}$, $p_{1/2}$, $f_{5/2}$, and $g_{9/2}$ orbits. For states below about 4 MeV, we found no significant differences between these results and the results found from calculation with the same Kuo-Brown interaction in either of our two more limited basis-vector spaces.

The Kuo-Brown interaction⁷ which we use includes contributions from renormalizations due to one-particle one-hole excitations of the core, as did the Kuo-Brown interaction derived earlier for the s - d shell.¹⁰ These Kuo-Brown interactions^{7,10} do not contain contributions from renormalizations due to two-particle excitations from the core, nor do they contain contributions associated with the excitation of two particles from the active orbits to orbits above the active ones. The Kuo interaction¹¹ for s - d -shell nuclei does contain contributions from these latter-types of excitation. (Also, it differs from the Kuo-Brown interaction in its bare matrix elements, before renormalization.) In s - d -shell calculations it has been found that many nuclear-structure results are very similar when either the Kuo-Brown¹⁰ interaction or the Kuo¹¹ interaction is used.⁸

The single-particle energies (s.p.e.) which we

use are the same as those used by Kuo and Brown in their calculation of the effective interaction (and in their calculations⁷ for ^{42}Ca). There is some uncertainty about the s.p.e. which should be used, especially for the $f_{5/2}$ and $g_{9/2}$ orbits. This uncertainty is indicated by the results from a $^{40}\text{Ca}(d,p)^{41}\text{Ca}$ experiment performed by Belote, Sperduto, and Buechner (BSB).¹² They concluded that in ^{41}Ca there is a significant splitting of the single-particle strength of every j orbit outside the ^{40}Ca core, except for $f_{7/2}$. The results of their analysis are shown in Table I, along with the s.p.e. used by Kuo and Brown. As Table I indicates, the $p_{3/2}$ strength was found to be split over two states, and the $p_{1/2}$ strength over five states. Spectroscopic factors S were deduced from the experimental data by distorted-wave analysis. These S values were normalized so that the spectroscopic factor to the $\frac{7}{2}^-$ ground state was unity. The normalized results suggest that only about half of the $f_{5/2}$ single-particle strength was observed, and less than 10% of the $g_{9/2}$ strength was observed. Recently, the strong transitions in the $^{40}\text{Ca}(d,p)^{41}\text{Ca}$ reaction were studied again, by Seth, Picard, and Satchler (SPS).¹³ Their purpose was to determine absolute spectroscopic factors for these transitions as accurately as possible. For transitions analyzed both by BSB¹² and SPS,¹³ the relative S values are in good agreement. The absolute values found by SPS are about 25% smaller than the values given by BSB. For the $f_{7/2}$, $p_{3/2}$, and $p_{1/2}$ orbits, the Kuo-Brown s.p.e. which we use are consistent with the centroids of single-particle strength as deduced from experiment. The $f_{5/2}$ and $g_{9/2}$ orbits are at a sufficiently high energy that they should have only a perturbative effect on the structure of low-lying states in the various calcium isotopes, and so the

TABLE I. Single-particle energies in ^{41}Ca . Column 2 shows the single-particle energy spectrum used by Kuo and Brown (see Ref. 7). Column 3 lists the centroids of the single-particle strengths observed in the $^{40}\text{Ca}(d,p)^{41}\text{Ca}$ experiment of Ref. 12. In column 4, $\sum S$ is the sum of the strengths determined from the distorted-wave analysis of the experimental data (see Ref. 12). Column 5 gives the number of levels over which the observed strength is spread.

Orbit	Kuo Brown (MeV)	Experiment (MeV)	$\sum S$	Number of levels
$f_{7/2}$	0	0	1.0	1
$p_{3/2}$	2.1	2.1	1.2	2
$p_{1/2}$	3.9	4.1	1.2	5
$f_{5/2}$	6.5	5.5	0.5	3
$g_{9/2}$	5.9	>5.0	0.1	1

uncertainty in the position of the s.p.e. for these two orbits should not be critical in the calculations discussed here.

The splitting of the single-particle strengths is one indication of the major imperfection of the models we are discussing. This major imperfection *vis-a-vis* nature is our neglect of breakup of the ^{40}Ca core. In ^{40}Ca itself, excited states are observed as low¹⁴ as 3.4 MeV; and these states necessarily involve configurations in which particles are excited out of the $A=40$ core. In their $^{40}\text{Ca}(d,p)^{41}\text{Ca}$ experiment, BSB¹² found evidence of 43 levels below 5.0-MeV excitation in ^{41}Ca ; but in our model, ^{41}Ca can have only five single-particle levels. One of the experimentally observed ^{41}Ca levels is a $\frac{3}{2}^+$ state near 2 MeV; this presumably involves core breakup. Indeed, as we shall show, in all the Ca isotopes up to at least ^{48}Ca , there appear to be observed states dominated by core-excited configurations at excitation energies as low as 2 or 3 MeV. Obviously, it would be desirable to include core-excited configurations in the calculations reported here. If we included them in the same way that we include the closed-core configurations, we would encounter prohibitively large matrices, and we would also encounter some problems associated with spurious center-of-mass motion. Some descriptions of core-excited states in ^{40}Ca , ^{41}Ca , and ^{42}Ca have been given by others.¹⁵⁻¹⁷

Because of the facts, (1) that the effective interaction we use is not designed for the same vector spaces that we use, and (2) that the experimental evidence clearly demonstrates a major deficiency of the models we use, we expect that our calculations can reproduce only a limited set of experimentally observed features. The best agreement is expected for the properties of those nuclear states which are dominated by $(f_{7/2}^{n_1} p_{3/2}^{n_2})$ configurations. Since in nature such states do mix with core-excited states, the spectroscopic strength which we calculate for *one* final nuclear state is likely to be spread, in nature, over *many* final nuclear states (some of them predominantly core-excited). If the core excitations in target state and final state are not similar, then this spreading effect will be particularly serious. However, it is reasonable to hope that these shell-model calculations can reproduce experimentally determined centroids for the $f_{7/2}$ and $p_{3/2}$ single-particle strengths. The model vector spaces are more seriously deficient for describing nuclear states dominated by configurations including $p_{1/2}$, $f_{5/2}$, and $g_{9/2}$ neutrons. And for such nuclear states, there are further theoretical difficulties: recall the above-discussed uncertainties in the s.p.e. for the $f_{5/2}$ and $g_{9/2}$ orbits. Thus for nu-

clear states dominated by $p_{1/2}$, $f_{5/2}$, and $g_{9/2}$ neutrons, one should expect only rough agreement between calculated results and experimentally observed results.

III. RESULTS OF CALCULATIONS WITH KUO-BROWN INTERACTION

In this section we present results for ^{42}Ca to ^{50}Ca calculated from the Kuo-Brown two-body interaction and single-particle energies. These calculations were performed in several alternative basis-vector spaces, and the results are presented graphically in Figs. 1–9. All these figures are set up with the same format. The first column, $f_{7/2}(H_{\text{expt}})$, shows the spectrum calculated using a vector space in which only pure- $f_{7/2}$ states are included, and this is the only theoretical column in Figs. 1–9 not calculated from the Kuo-Brown interaction. Instead, this set of spectra was calculated by using the effective two-neutron interaction taken directly from the observed spectrum of ^{42}Ca . Thus, in these results the effects of all orbits other than $f_{7/2}$ are introduced implicitly via the empirically determined effective interaction. The second column, $f_{7/2}\text{-KB}$, shows the spectrum calculated by using a vector space which again includes only pure- $f_{7/2}$ states, but with the effective interaction defined by the $\langle f_{7/2}^2 J | V | f_{7/2}^2 J \rangle$ matrix elements of the Kuo-Brown interaction. In principle then, this $f_{7/2}\text{-KB}$ spectrum completely excludes the effects of configurations with particles in the $p_{3/2}$, $p_{1/2}$, $f_{5/2}$, and $g_{9/2}$ orbits. The third column, $f_{7/2}\text{-}p_{3/2}$, shows the spectrum obtained when the model space includes all states of all configurations $f_{7/2}^{n_1} p_{3/2}^{n_2}$, and when the effective Hamiltonian is defined by those one- and two-body matrix elements of the Kuo-Brown Hamiltonian involving only the $f_{7/2}$ and/or $p_{3/2}$ orbits. The fourth column, $f\text{-}p$, shows the spectrum obtained when all four $f\text{-}p$ -shell orbits are active, and when the Hamiltonian is defined by the Kuo-Brown matrix elements for these four shells (but the number of particles distributed among the $p_{1/2}$ and $f_{5/2}$ orbits is ≤ 2 , as explained in Sec. II). The last column, $f\text{-}p\text{-}g$, shows the spectrum obtained when all four $f\text{-}p$ -shell orbits and also the $g_{9/2}$ orbit are active (subject to the two-particle excitation restriction discussed above), and when the Hamiltonian is defined by all the Kuo-Brown matrix elements.

In general, for the theoretical spectra in Figs. 1–9, all levels calculated below 5 MeV are shown. (In a few instances, 0^+ states calculated to be above this energy are also shown.) We have calculated only positive-parity states for even- A nuclei and only negative-parity states for odd- A

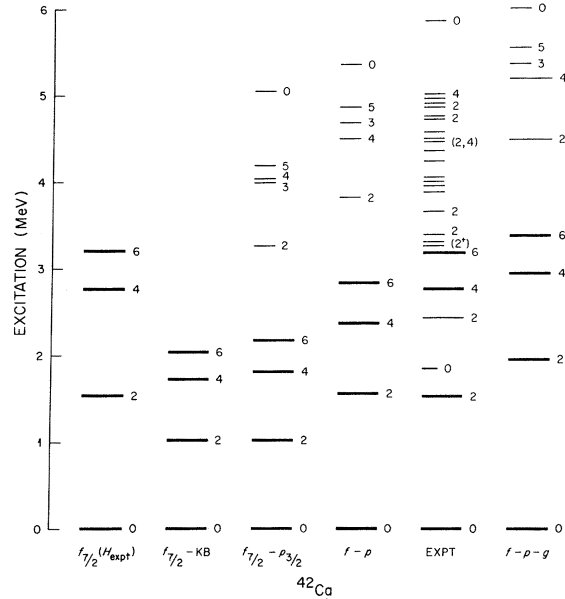


FIG. 1. Calculated and experimental excitation energies in ^{42}Ca . The column labels are explained in Sec. III. The experimental excitation energies are taken from Ref. 21. In the experimental spectrum, all known possible even-parity levels below 5.0 MeV are shown. The levels indicated with long lines are calculated or observed to be populated strongly in the $^{43}\text{Ca}(d,t)^{42}\text{Ca}$ reaction. The experimental data on the $^{43}\text{Ca}(d,t)^{42}\text{Ca}$ reaction are found in Ref. 22.

nuclei. For this reason, we generally omit parity assignments from all the theoretical spectra in the figures in this paper. For odd- A nuclei we show $2J$ for each level in both the theoretical and experimental spectra. In those cases where there are multiple spin assignments made for a given level in a theoretical spectrum, we mean that there is a level for each indicated spin at the given energy. In most cases, only the lowest four states with a given J value were calculated. Thus in spectra where the first four eigenvalues for a given spin lie below 5 MeV, there may be more theoretical states with that J value which would lie below 5 MeV. The exception to this general rule is that eight $\frac{5}{2}^-$ and eight $\frac{1}{2}^-$ states were calculated for ^{43}Ca and ^{45}Ca , and for these nuclei the calculated positions of all $\frac{1}{2}^-$ and $\frac{5}{2}^-$ states below 5.0 MeV are shown. These higher $\frac{1}{2}^-$ and $\frac{5}{2}^-$ states were generated so that by calculating spectroscopic factors for these states, we could see whether there was any significant calculated $p_{1/2}$ or $f_{5/2}$ single-particle strength below 5-MeV excitation in ^{43}Ca and ^{45}Ca . (Most of the $f_{7/2}$ and $p_{3/2}$ strength calculated for the odd isotopes lies within the first four $\frac{7}{2}^-$ states and the first four $\frac{3}{2}^-$ states.) Obviously, the pure- $f_{7/2}$ model is mean-

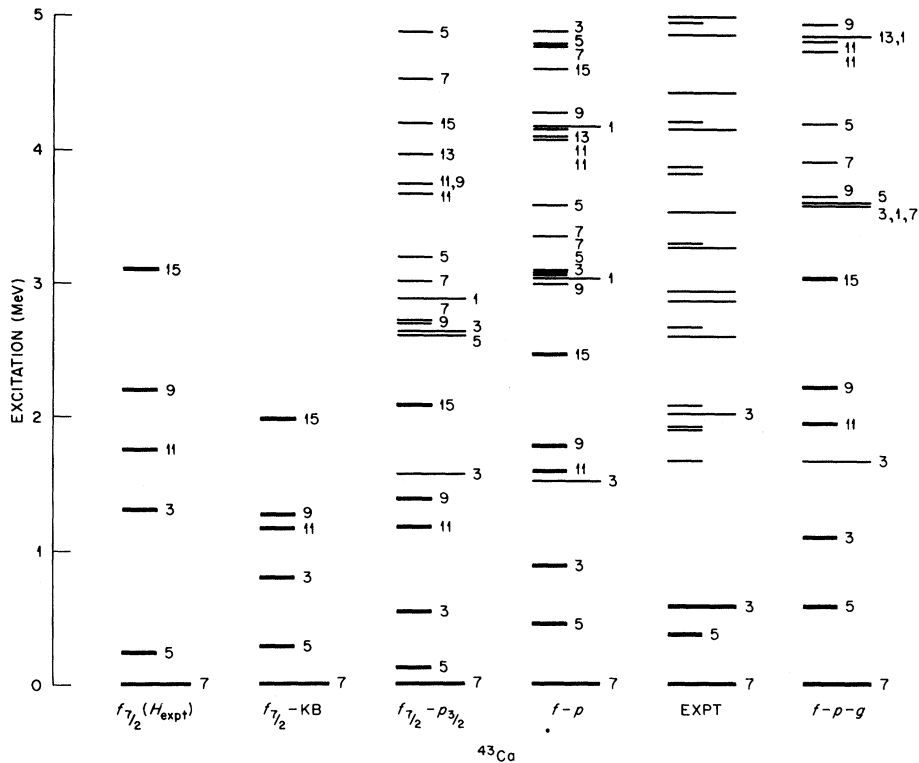


FIG. 2. Calculated and experimental excitation energies in ^{43}Ca . The column labels are explained in Sec. III. Experimental information in this figure is taken from Ref. 24. In the experimental spectrum, all known possibly odd-parity levels below 2.0 MeV are shown. Above 2.0 MeV in the experimental spectrum, only those levels which are populated with $l=1$ or $l=3$ transfers in the $^{42}\text{Ca}(d,p)^{43}\text{Ca}$ reaction are shown. The levels indicated with long lines are calculated or observed to be populated strongly in the $^{42}\text{Ca}(d,p)^{43}\text{Ca}$ reaction.

ingless for ^{49}Ca and ^{50}Ca , and so the pure- $f_{7/2}$ spectra are omitted from the figures drawn for these nuclei.

The levels calculated in the pure- $f_{7/2}$ model, and their modified versions as calculated in the larger spaces, will be referred to as " $f_{7/2}$ levels." These levels are drawn as extra-thick lines in Figs. 1-7. The $f_{7/2}$ levels, at least, should be reasonably well reproduced by the calculations.

In addition to information on the energies of states in $^{42-50}\text{Ca}$, the figures also contain some information on single-particle strengths for those isotopes which can be reached with single-neutron stripping reactions - i.e., $^{42-45}\text{Ca}$, ^{47}Ca , and ^{49}Ca . In the figures for these nuclei, levels which are populated with significant strength in the stripping reactions are indicated with long lines, while other levels are indicated by short lines. Numerical values for the spectroscopic factors in neutron transfer reactions are summarized in Tables III-XI. These tables will be discussed in more detail later.

We first discuss the general characteristics of the various calculated spectra. As already ex-

plained, the first two columns in the figures for ^{42}Ca - ^{46}Ca show pure- $f_{7/2}$ -shell-model results. Column one, $f_{7/2}(H_{\text{expt}})$, uses the effective interaction specified by the observed energies of the lowest 0^+ , 2^+ , 4^+ , and 6^+ states in ^{42}Ca . Thus it implicitly includes the effects of all other orbits on the energies of the low-lying states. The calculation $f_{7/2}$ -KB explicitly excludes effects due to the other three orbits in the f - p shell, and due to the $g_{9/2}$ orbit. As is well known, the $f_{7/2}(H_{\text{expt}})$ calculation is in rather good agreement with the observed spectrum of low-lying states in $^{42-46}\text{Ca}$. In all five of these isotopes, the ordering of spins is the same in columns $f_{7/2}$ -KB and $f_{7/2}(H_{\text{expt}})$, but the spectra for $f_{7/2}$ -KB is compressed relative to that of $f_{7/2}(H_{\text{expt}})$. This compression implies that one or more of the neglected orbits $p_{3/2}$, $f_{5/2}$, $p_{1/2}$, $g_{9/2}$ plays a significant role in affecting the observed excitation of low-lying states in ^{42}Ca - ^{46}Ca .

Columns 3, 4, and 6 in Figs. 1-5 show what happens when orbits above $f_{7/2}$ are added to the active space. The biggest change occurs when we add the $p_{3/2}$ orbit to the active-model space, i.e., when we go from a pure- $f_{7/2}$ model to an $f_{7/2}$ - $p_{3/2}$

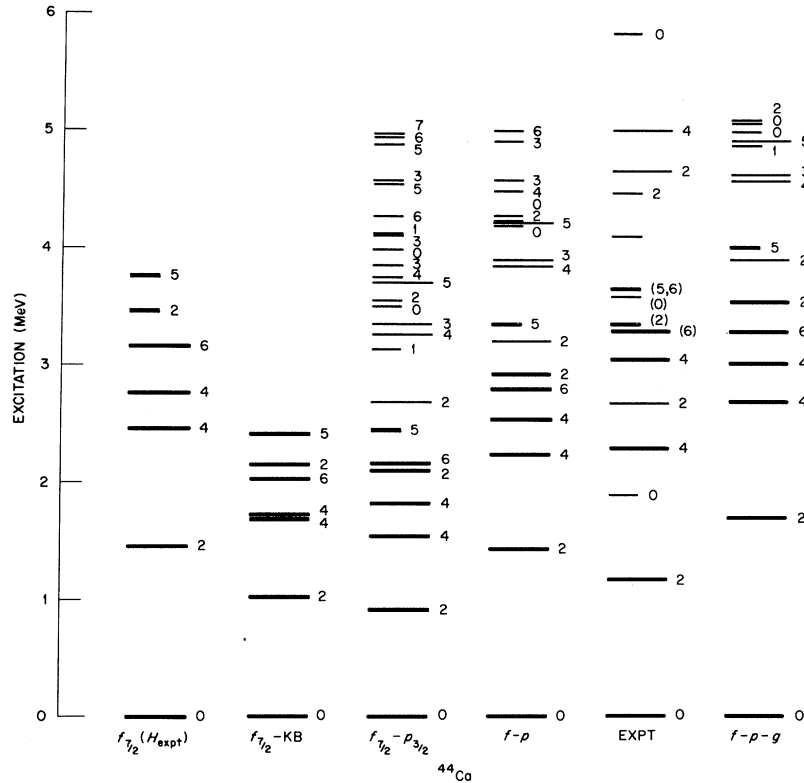


FIG. 3. Calculated and experimental excitation energies for ^{44}Ca . The column labels are explained in Sec. III. The experimental information is taken from Refs. 23 and 26. In the experimental spectrum, all known possibly even-parity levels below 3.0 MeV are shown. Between 3.0 and 5.0 MeV, all levels observed to be populated in the $^{43}\text{Ca}(d,p)^{44}\text{Ca}$ reaction with $l=1$ or $l=3$ transitions, or for which spin assignments are known from the $^{42}\text{Ca}(t,p)^{44}\text{Ca}$ reaction, are shown. The levels drawn with long lines are calculated or observed to be populated strongly in the $^{43}\text{Ca}(d,p)^{44}\text{Ca}$ reaction.

model. Then there is a large increase in the number of levels below 5 MeV. But the calculated $f_{7/2}-p_{3/2}$ spectra are still too compressed with respect to the experimental spectrum. The spectra labeled $f-p$ contain the perturbative corrections (to predominantly $f_{7/2}-p_{3/2}$ states) due to raising neutron pairs up to the $p_{1/2}$ and/or $f_{5/2}$ orbits. The main effect is an expansion compared to the $f_{7/2}-p_{3/2}$ spectra, and this expansion gives closer agreement with experiment. The level orderings are very similar in the two calculations $f_{7/2}-p_{3/2}$ and $f-p$. When the vector spaces are further enlarged, as in the $f-p-g$ calculation, then the spectra are further expanded.

It can be seen from the energy-level plots of $^{42-46}\text{Ca}$ that the low-lying excitation spectra obtained in the $f-p$ and $f-p-g$ calculations could have been obtained in the $f_{7/2}-p_{3/2}$ calculation by slightly increasing the strengths of all the $f_{7/2}-p_{3/2}$ matrix elements. In the $f-p-g$ calculation, the expansion of the spectra overshoots the mark, with respect to the experimental spectra. To make this effect readily apparent, we have placed the experiment-

ally observed spectrum between the $f-p$ spectrum and the $f-p-g$ spectrum. One can then see that if one constructed spectra by averaging the excitation energies of analogous states in the $f-p$ and $f-p-g$ spectra, the averaged spectra would be in general agreement with the experimentally observed spectra below about 3 MeV. Exceptions are the second 0^+ and second 2^+ states in ^{42}Ca , ^{44}Ca , and ^{46}Ca , and a few states of uncertain spin and parity in the odd isotopes. We shall say more about these states later.

It seems to us that a better treatment of the $g_{9/2}$ orbit could lead to a directly calculated shell-model spectrum similar to the intermediate (averaged) spectrum. As we indicated in Sec. II, the position of the $g_{9/2}$ s.p.e. is very uncertain from an experimental point of view. It is possible that the centroid of the $g_{9/2}$ single-particle strength lies at an energy higher than the 5.9 MeV that was used by Kuo and Brown, and by us. By treating this $g_{9/2}$ s.p.e. as an adjustable parameter, and by raising it to a higher energy, we could decrease its contribution to the calculation, and

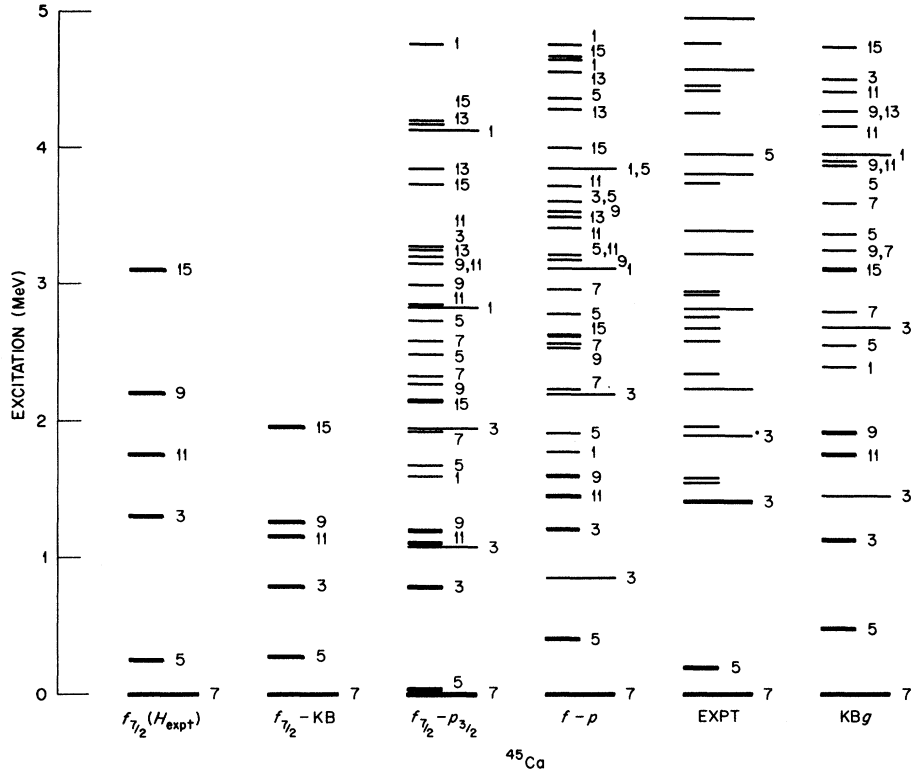


FIG. 4. Calculated and observed excitation spectra for ^{45}Ca . The column labels are explained in Sec. II. The experimental information in this figure is taken from Ref. 30. In the experimental spectrum all known possibly odd-parity states below 3.0 MeV are shown, and between 3.0 and 5.0 MeV all states observed to be populated with $l=1$ or $l=3$ transitions in the $^{44}\text{Ca}(d,p)^{45}\text{Ca}$ reaction are shown. The levels drawn with long lines are calculated or observed to be populated strongly in the $^{44}\text{Ca}(d,p)^{45}\text{Ca}$ reaction.

thus compress the f - p - g spectra. Raising this $g_{9/2}$ s.p.e. would also affect the calculation of the effective interaction.

In addition to the uncertainty of the $g_{9/2}$ s.p.e., there is the possibility that in the Kuo-Brown interaction, the two-body matrix elements of the type $\langle j_1 j_2 J | V | g_{9/2}^2 J \rangle$ may be less accurate than the other matrix elements which do not involve $|g_{9/2}^2 J \rangle$ states. This possibility was pointed out by Kuo and Brown.⁷ A distinguishing feature of these $\langle j_1 j_2 J | V | g_{9/2}^2 J \rangle$ matrix elements is that the three-particle one-hole renormalization contribution for these matrix elements involves matrix elements between odd-parity particle-hole states. There are very collective low-lying negative-parity states observed in ^{40}Ca , and it is not clear how well these states can be described by the limited set of one-particle one-hole core excitations implied in the Kuo-Brown prescription for renormalization of two-body matrix elements.

For the isotopes from ^{42}Ca to ^{46}Ca , the excitation spectrum intermediate to the calculated f - p and f - p - g spectra gives reasonable agreement with the experimentally observed low-lying exci-

tation spectra. The quality of the agreement is not as good as that obtained in the several previous calculations (discussed in the Introduction)⁴⁻⁶ which included $p_{3/2}$ -orbit contributions, and which used interactions obtained by a many-parameter fit to observed energies. But, in general, for ^{42}Ca - ^{45}Ca there are no great differences in the quality of agreement obtained from these earlier calculations and from the averaged f - p and f - p - g calculations. Beyond ^{46}Ca , however, there is not good agreement between our "averaged" spectra and the observed spectra. For example, in the observed spectrum of ^{47}Ca , there is a 2-MeV gap between the $\frac{7}{2}^-$ ground state and the $\frac{3}{2}^-$ first excited state. But in the f - p model spectrum for ^{47}Ca , the first $\frac{3}{2}^-$ and the first $\frac{7}{2}^-$ states are almost degenerate, and there are six states below 2 MeV. The matrix dimensions of the f - p - g calculation for ^{47}Ca are too large to handle. We have not investigated whether the inclusion of $g_{9/2}$ excitations would give a big improvement over the f - p model for ^{47}Ca , but we do not expect that it would. In ^{48}Ca , we see again that the f - p model gives excited states which are too low with re-

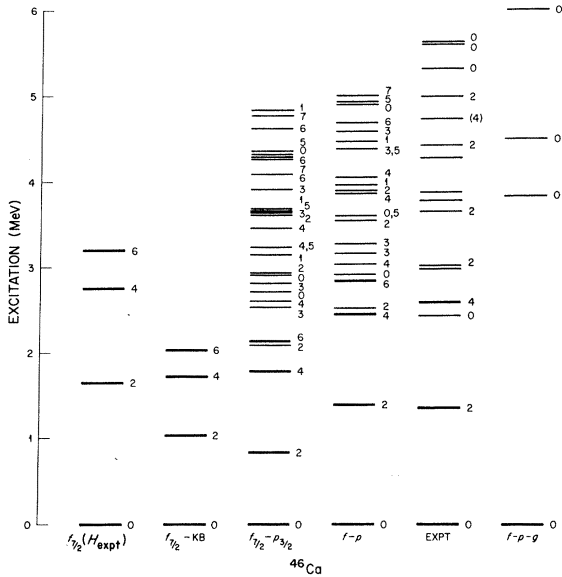


FIG. 5. Calculated and observed excitation spectra for ^{46}Ca . The column labels are explained in Sec. III. The experimental spectrum is taken from Ref. 23. In the experimental spectrum, all known possibly even-parity states below 5.0 MeV are shown, and in addition the known 0^+ states between 5.0 and 6.0 MeV are shown.

spect to experiment by roughly 2 MeV. In this case it is possible to calculate the 0^+ states in the f - p - g space. The results, shown in Fig. 7, indicate that such $g_{9/2}$ excitations cannot account for the discrepancies from observed spectra; for even though the inclusion of $g_{9/2}^2$ excitations increases the separation of the lowest two 0^+ states, the second 0^+ state is still significantly lower than the second observed 0^+ state. This feature — that the excited states are calculated to be too low relative to the ground state — persists in ^{49}Ca .

The first question one might ask when faced with these results is: Why does the general quality of the agreement between theory and experiment change abruptly from ^{46}Ca to ^{47}Ca ? There is one fairly obvious answer. As shown by Figs. 1–5, the pure- $f_{7/2}$ calculation $f_{7/2}(H_{\text{expt}})$ gives quite reasonable agreement with experiment for a number of the levels with known spin in ^{42}Ca to ^{46}Ca . To a first approximation then, the low-lying levels in these nuclei consist of pure- $f_{7/2}^n$ configurations. The spectra of these states are affected primarily by the matrix elements $\langle f_{7/2}^2 J | V | f_{7/2}^2 J \rangle$, and are less sensitive to the other two-body matrix elements and to the single-particle energies. In the ^{47}Ca vector space there is only one pure- $f_{7/2}^n$ basis state; it has $J^\pi = \frac{7}{2}^-$, and it is the dominant component of the ground state. All higher calculated states are therefore dominated by excitations to the remaining active orbits in the cal-

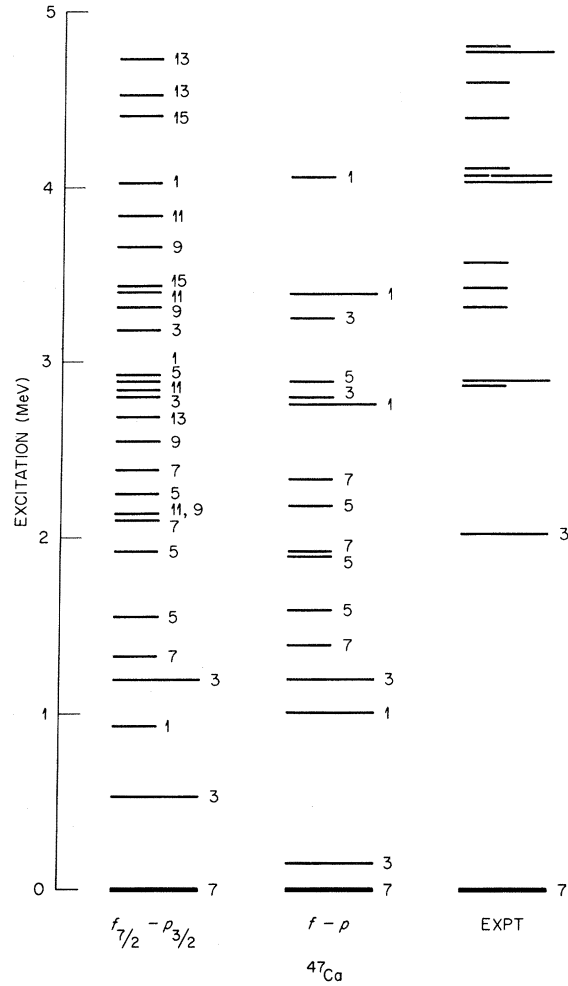


FIG. 6. Calculated and observed excitation spectra for ^{47}Ca . The column labels are explained in Sec. III. The experimental information is taken from Refs. 31 and 32. In the experimental spectrum, all known possibly odd-parity states below 5.0 MeV are shown. The levels drawn with long lines are calculated or observed to be populated strongly in the $^{46}\text{Ca}(d, p)^{47}\text{Ca}$ reaction.

ulation. Therefore the positions of these higher calculated states are sensitive to matrix elements other than the $f_{7/2}^2$ matrix elements, and sensitive to the s.p.e. of the higher orbits. Thus by assuming that the Kuo-Brown $f_{7/2}^2$ matrix elements are “almost correct,” while the remaining matrix elements are less accurate, we can “explain” the success of the calculation in reproducing low-lying spectra of the isotopes ^{42}Ca through ^{46}Ca , and the contrasting failure to accurately reproduce the low-lying spectra of ^{47}Ca – ^{50}Ca .

As we shall demonstrate in the next section, we have found that an improvement in the calculated spectra, at least for ^{47}Ca and ^{48}Ca , can be achieved by either of two relatively simple procedures.

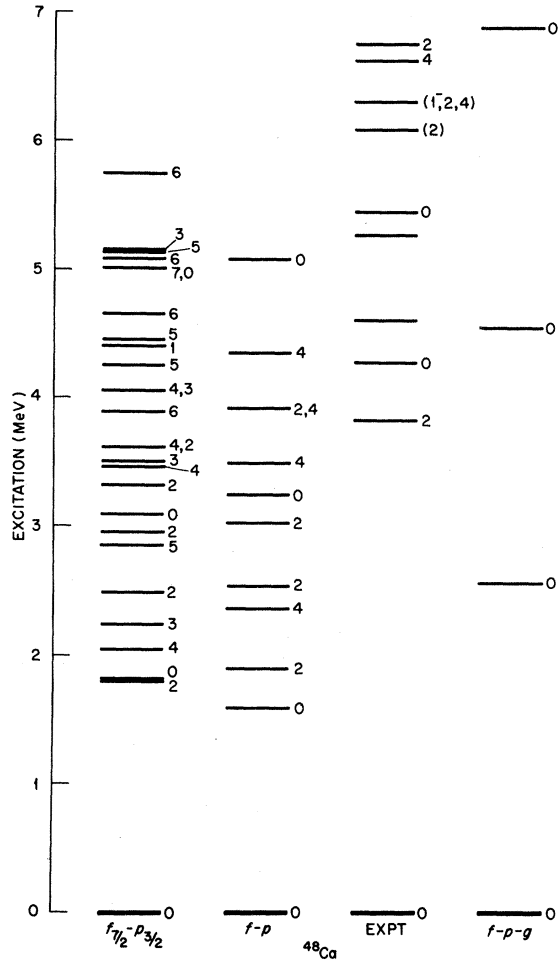


FIG. 7. Calculated and observed excitation spectra for ^{48}Ca . The column labels are explained in Sec. III. The experimental spectrum is taken from Refs. 21 and 23. In the experimental spectrum, all known possibly even-parity states below 7.0 MeV are shown.

One procedure is to use a larger $f_{7/2}-p_{3/2}$ single-particle splitting for the heavier isotopes than is used for the lighter isotopes. This choice was made by Sartoris and Zamick¹⁸ in a calculation of ^{47}Ca . They found that a splitting of roughly 3 MeV in ^{47}Ca gives significant improvement in the agreement between calculation and experiment for these heavier calcium isotopes. But a similar improvement can be achieved while keeping the effective Hamiltonian constant for all the isotopes, by altering the Kuo-Brown two-body matrix elements $\langle f_{7/2} p_{3/2} J | V | f_{7/2} p_{3/2} J \rangle$. The interaction energy of a $p_{3/2}$ particle with the state $|f_{7/2}^n J=0\rangle$ is given by

$$n \frac{\sum_J (2J+1) \langle f_{7/2} p_{3/2} J | V | f_{7/2} p_{3/2} J \rangle}{\sum_J (2J+1)} \equiv C_{7/2,3/2}. \quad (1)$$

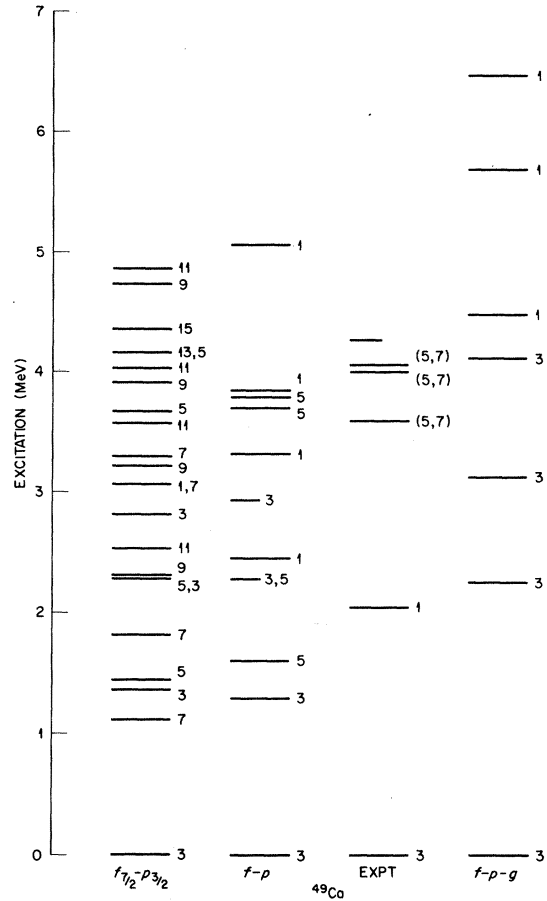


FIG. 8. Calculated and observed excitation spectra for ^{49}Ca . The column labels are explained in Sec. III. The experimental information is taken from Ref. 34. In the experimental spectrum, all known possibly odd-parity states below 5.0 MeV are shown. The levels drawn with long lines are calculated or observed to be populated strongly with $l=1$ or $l=3$ transitions in the $^{48}\text{Ca}(d,p)^{49}\text{Ca}$ reaction.

The energy $C_{7/2,3/2}$ is called the "center of gravity" of the $f_{7/2}-p_{3/2}$ interaction. From (1), together with the fact that for $^{40-47}\text{Ca}$ the ground states are predominantly $f_{7/2}^n$, we see that the position of the $p_{3/2}$ single-particle strength in a given odd nucleus becomes more sensitive to this center of gravity $C_{7/2,3/2}$ as the number of $f_{7/2}$ particles increases. We have found that in ^{47}Ca , a 250-keV shift in this center of gravity shifts the single-particle strength by 1.5 MeV with respect to the ground state. As we shall show in Sec. IV, an upward shift of the $f_{7/2}-p_{3/2}$ interaction matrix elements (i.e., a weakening of the $f_{7/2}-p_{3/2}$ attraction) leads to significant improvement in the agreement of theory and experiment for the spectra of the heavier isotopes, $^{48}\text{Ca}-^{50}\text{Ca}$. However, because n is small for the lighter calcium isotopes, and be-

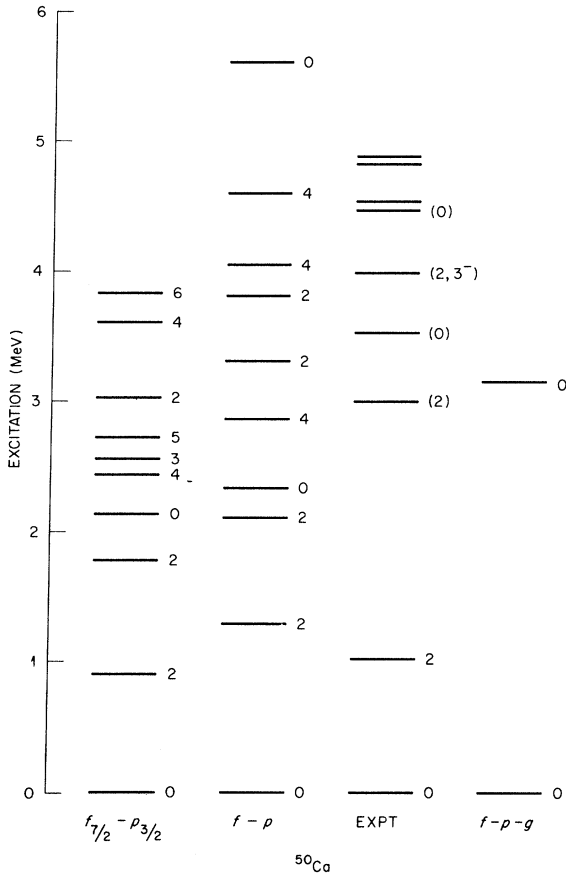


FIG. 9. Calculated and observed excitation spectra for ^{50}Ca . The column labels are explained in Sec. III. The experimental information is taken from Ref. 23. In the experimental spectrum, all known possibly even-parity states below 5.0 MeV are shown.

cause most of the low-lying states in ^{42}Ca to ^{46}Ca are dominated by $f_{7/2}$ configurations, we find that a shift of 250 keV in $C_{7/2,3/2}$ has little effect on the calculated structure of the low-lying states in ^{42}Ca – ^{46}Ca .

It is possible also to make plausible arguments justifying the use of different single-particle energies for the light and heavy Ca isotopes. The single-particle energies are commonly viewed as representing the interaction of the active particles with the inert ^{40}Ca core which we assume. We know that the calcium isotopes do not really have an inert ^{40}Ca core; i.e., there is significant excitation of particles out of the core and into the f - p shell. There are seven more particles in ^{48}Ca than in ^{41}Ca . Because of these extra seven particles, the distribution of the original "core" particles is altered from what it is in ^{41}Ca ; and so it seems reasonable that the effective interaction of an active particle with the 40 core particles

should be different in ^{41}Ca and ^{48}Ca . An A -dependent single-particle energy is, of course, a special kind of many-body operator. Indeed, if in the calculation of the effective interaction all possible renormalization diagrams up to second order were included exactly, then such A -dependent effects would be taken into account properly, to second order. (Thus the second-order "blocking" effects would be taken into account.) But Kuo and Brown neglected some second-order renormalization terms; e.g., they neglected the three-body contribution. Furthermore, they ignored renormalization corrections higher than second order. Hence it seems plausible that some of the shortcomings in the calculation of the Kuo-Brown interaction could be approximately compensated for by A -dependent changes in the single-particle energies.

On the other hand, it is not unreasonable to suspect that an improved calculation of the $f_{7/2}$ - $p_{3/2}$ two-body matrix elements might differ from the Kuo-Brown matrix elements by 200 or 300 keV. We do not find any distinctive feature of the shell-model results which definitively favors either one of the two means of improvement we have mentioned.

In summary, the energy-level spectra calculated from the Kuo-Brown effective Hamiltonian are in reasonable agreement with experiment for the $f_{7/2}$ levels in ^{42}Ca to ^{46}Ca , and for the low-lying $\frac{3}{2}^-$ states in ^{43}Ca and ^{45}Ca . The agreement is not good for ^{47}Ca to ^{50}Ca . However, much better agreement can be achieved with relatively simple changes of the effective Hamiltonian – as we shall show in the next section, by presenting results from a specific modification of the Kuo-Brown Hamiltonian.

IV. RESULTS OF CALCULATIONS WITH A MODIFIED VERSION OF THE KUO-BROWN INTERACTION

In this section we discuss in detail the results of calculations with a modified version of the Kuo-Brown Hamiltonian. This modified version which we shall call KB', was obtained by changing some of the two-body matrix elements to which the calculated energy spectra are most sensitive. The changes were suggested by the results presented in the last section. When we use the modified Hamiltonian KB' in the four-shell f - p vector space, we get shell-model results which are in good agreement with the experimentally observed excitation energies and strength distributions of the $f_{7/2}$ states, and with the experimentally observed centroids of the strong $p_{3/2}$ single-particle strengths. The results from this calculation also suggest that at excitation energies ≥ 2.5 MeV, core excitation

is important at least in all the isotopes of calcium with $A = 42$ to 48 . The evidence for this importance is: (1) That above 2.5 -MeV excitation in the odd calcium isotopes, the calculated density of states is significantly less than the observed density; and (2) that in ^{42}Ca , ^{44}Ca , and ^{46}Ca the second 0^+ and second 2^+ states apparently cannot be accounted for in the vector spaces we have used.

The rest of this section will be organized as follows. First, we describe the way in which we obtained the modified Hamiltonian KB' . Second, we explain our reasons for choosing this way of modifying the Kuo-Brown interaction, and we mention some alternative ways. Third, we discuss in detail the energy spectra and single-nucleon spectroscopic factors calculated for $^{42-50}\text{Ca}$ from KB' . Finally, we briefly compare the KB' interaction, and its shell-model results, with some interactions and results of (a) previous studies by other workers, and (b) a further exploratory study of our own.

The shell-model vector space used in the calculations described in this section is identical to the space we have been calling f - p : Its active nucleons are restricted to the four single-particle orbits of the f - p shell, and its configurations comprise those with a total of no more than two particles in the $p_{1/2}$ and $f_{5/2}$ orbits. To specify the model Hamiltonian KB' , we use all the matrix elements of the Kuo-Brown effective interaction, with these eight exceptions: the four matrix elements $\langle f_{7/2}^2 J | V | f_{7/2}^2 J \rangle$ with $J = 0, 2, 4$, and 6 ; and the four matrix elements $\langle f_{7/2} p_{3/2} J | V | f_{7/2} p_{3/2} J \rangle$ with $J = 2, 3, 4$, and 5 . The four pure- $f_{7/2}$ matrix elements were treated as adjustable parameters in a least-squares search to find the best fit to a selected set of experimentally observed levels.¹⁹ At first we searched with all eight of the aforementioned parameters as adjustable parameters. But convergence was poor. Apparently, the four $f_{7/2}$ - $p_{3/2}$ matrix elements could not all be accurately determined by the set of observed levels included in the search. (This set is described below.) The general trend of this eight-parameter search was to raise the center of gravity $C_{7/2,3/2}$ by about 0.3 MeV. We finally decided to fix three of the four $f_{7/2}$ - $p_{3/2}$ matrix elements at values obtained at an intermediate (i.e., unconverged) stage of this eight-parameter search. We fixed the values of the three matrix elements $\langle f_{7/2} p_{3/2} J | V | f_{7/2} p_{3/2} J \rangle$ with $J = 2, 3$, and 4 ; but we allowed the $J = 5$ matrix element to remain a free parameter. We then searched up to convergence with five free parameters: the $J = 5$ matrix element, and the four pure- $f_{7/2}$ matrix elements. The set of 25 observed levels fitted included all the known " $f_{7/2}$ levels", the second $\frac{3}{2}^-$ levels in

^{43}Ca and ^{45}Ca , the first $\frac{3}{2}^-$ level in ^{47}Ca , and the ground-state energies of ^{49}Ca and ^{50}Ca with respect to ^{40}Ca . The search was made for ground-state binding energies (relative to ^{40}Ca) and excitation energies. The single-particle energies were held fixed at the Kuo-Brown values. The converged solution of this five-parameter search constitutes the modified interaction which we call KB' . In Table II we list those matrix elements of the modified interaction which involve the $f_{7/2}$ and $p_{3/2}$ orbits. This list includes all the matrix elements which are different from those in the Kuo-Brown interaction. Table II also lists the corresponding matrix elements calculated by Kuo and Brown,⁷ and those obtained by Engeland and Osnes⁵ in their least-squares search for an effective interaction, and those obtained by Federman and Talmi⁶ in their least-squares search.

We next comment on our reasons for choosing the general *kind* of modifications we have made to the Kuo-Brown interaction. (Our comments here are a continuation of the discussion in the last three paragraphs of Sec. II.) In the models we have used, most of the low-lying states in the calcium isotopes are dominated by pure- $f_{7/2}$ configurations. Thus the pure- $f_{7/2}$ matrix elements are the most important in determining the properties of the low-lying states, and it is reasonable to try to adjust these first. The aim is to make up for faults in the derivation of the Kuo-Brown interaction, and also to make up for the fact that we use the Kuo-Brown interaction in a limited version of the shell-model space for which it was designed. In particular, we hope to make up for the neglect of active $g_{9/2}$ particles in our explicit shell-model basis states. The adjustment of these $f_{7/2}$ matrix elements was determined by requiring a least-squares fit to observed energy levels. That seems a reasonable criterion. The next-most-important configurations, after the pure- $f_{7/2}^n$ configurations, are the $f_{7/2}^{n-1} p_{3/2}$ configurations. Thus the next-most-important two-body matrix elements to alter would be $\langle f_{7/2} p_{3/2} J | V | f_{7/2} p_{3/2} J \rangle$ and $\langle f_{7/2}^2 J | V | f_{7/2} p_{3/2} J \rangle$. Of these, only the matrix elements $\langle f_{7/2} p_{3/2} J | V | f_{7/2} p_{3/2} J \rangle$ affect the centroid energy of $f_{7/2}^{n-1} p_{3/2}$ states. (The matrix elements $\langle f_{7/2}^2 J | V | f_{7/2} p_{3/2} J \rangle$ enter into the *width* of the $f_{7/2}^{n-1} p_{3/2}$ centroid.) Our results from the f - p calculation, as described in the preceding section, pointed to the necessity of raising the position of the $p_{3/2}$ single-particle strength in ^{47}Ca . As discussed previously, this needed change can be effected in at least two simple ways - by changing the two-body matrix elements $\langle f_{7/2} p_{3/2} J | V | f_{7/2} p_{3/2} J \rangle$, or by changing the single-particle energies as a function of A . We have chosen to investigate the first-mentioned

TABLE II. Matrix elements $\langle j_1 j_2 J | V | j_3 j_4 J \rangle$ which involve only $f_{7/2}$ and/or $p_{3/2}$ orbits. The units are MeV. The first two columns of matrix elements are taken from the indicated references. Entries in the column headed KB are matrix elements calculated by Kuo and Brown (see Ref. 7). Entries in the column headed KB' are those in the modified Kuo-Brown interaction described in our text.

$2j_1$	$2j_2$	$2j_3$	$2j_4$	J	Engeland and Osnes ^a (MeV)	Federman and Talmi ^b (MeV)	KB	KB'
7	7	7	7	0	-3.12	-2.64	-1.81	-2.11
				2	-0.89	-0.83	-0.78	-1.11
				4	-0.17	-0.20	-0.09	-0.10
				6	+0.17	+0.28	+0.23	+0.23
7	7	7	3	2	-0.94	-0.74	-0.50	-0.50
				4	-0.56	-0.35	-0.31	-0.31
7	3	7	3	2	-2.04	-1.98	-0.86	-0.56
				3	0.28	+1.98	-0.03	+0.25
				4	-0.50	-0.93	-0.05	+0.28
				5	-1.69	+0.59	+0.15	+0.49
7	7	3	3	0	...	-1.64	-0.78	-0.78
				2	...	-1.20	-0.27	-0.27
7	3	3	3	2	...	+0.60	-0.32	-0.32
3	3	3	3	0	...	-1.40	-1.21	-1.21
				2	...	0	-0.38	-0.38

^aSee Ref. 5.

^bSee Ref. 6.

way: changing the two-body matrix elements.

As an alternative to adjusting the Kuo-Brown interaction "empirically" via a least-squares search to observed levels, we could instead adjust it analytically via the Kuo-Brown renormalization procedure. In this kind of analytic adjustment (unlike the least-squares adjustment), there would be no thought of compensating for "errors" in the Kuo-Brown calculation, or of compensating for our restriction to a total of two or fewer $f_{5/2}$ and $p_{1/2}$ neutrons. Instead, the idea would be simply to make up for our neglect of active $g_{9/2}$ particles in the shell-model basis states. One procedure would be to redo the renormalization part of the Kuo-Brown calculation so as to include perturbations of the two-body f - p -shell matrix elements by $g_{9/2}^2$ excitations as well as by other $2\hbar\omega$ corrections. In fact, we have carried out this procedure. We compared the resulting f - p -shell matrix elements with the corresponding Kuo-Brown matrix elements, and found the two sets extremely similar. Furthermore, when we calculated the spectra of the calcium isotopes with the new matrix elements in the f - p space, we found that the calculated spectra were essentially identical with results obtained from the Kuo-Brown interaction. As we showed in Sec. III, when the $g_{9/2}$ orbit is allowed to be active in the shell-model space, it has an important effect on the calculated spectra. But now we see that when $g_{9/2}$ contributions are in-

cluded only implicitly, via second-order renormalizations of the two-body matrix elements, they have no significant effect on the calculated spectra. Obviously, these second-order renormalizations are insufficient. The reason is that they entail the use of "bare" $\langle j_1 j_2 J | V | g_{9/2}^2 J \rangle$ matrix elements – and these are quite different from renormalized $\langle j_1 j_2 | V | g_{9/2}^2 J \rangle$ matrix elements. What we need are the *higher-order* effects that would be introduced by using renormalized $\langle j_1 j_2 | V | g_{9/2}^2 J \rangle$ matrix elements to perturb the f - p -shell matrix elements. We shall explain this more fully in the next paragraph.

In the Kuo-Brown matrix element $\langle f_{7/2}^2 J=0 | V | g_{9/2}^2 J=0 \rangle$, the contribution from the bare matrix element is 0.6 MeV, and the contribution from the renormalization correction is 2.0 MeV. Of the 20 matrix elements $\langle j_1 j_2 J | V | g_{9/2}^2 J \rangle$ in the Kuo-Brown interaction, there are nine for which the renormalization contribution exceeds the contribution of the bare matrix element. Thus, when $g_{9/2}$ orbit is treated as active in the shell-model calculation, a considerable part of its effect on low-lying structure comes about from large core-polarization contributions in the effective interaction of active $g_{9/2}$ nucleons with other active nucleons. But when the $g_{9/2}$ orbit is not treated as active, and when its effects are introduced as second-order perturbations calculated with bare matrix elements, then the large core-polarization effects on the $g_{9/2}$ orbit are not included at all.

One remedy is to renormalize in a different way – by starting with the set of matrix elements derived by Kuo and Brown for use in shell-model calculations employing the full five-shell space, and then using second-order perturbation theory within this set so as to adjust for omission of $g_{9/2}$ particles from the shell-model basis. To be

$$\langle j_1 j_2 \mathcal{J} | V | j_3 j_4 \mathcal{J} \rangle_4 = \langle j_1 j_2 \mathcal{J} | V | j_3 j_4 \mathcal{J} \rangle_5 - \frac{\langle j_1 j_2 \mathcal{J} | V | g_{9/2}^2 \mathcal{J} \rangle_5 \langle g_{9/2}^2 \mathcal{J} | V | j_3 j_4 \mathcal{J} \rangle_5}{\Delta},$$

For the case of the diagonal matrix elements, Δ is uniquely defined as $E(g_{9/2}^2) - E(j_1 j_2)$, where $E(j j')$ is the sum of single-particle energies for orbits j and j' . For the off-diagonal matrix elements, some arbitrary assumption for this denominator must be made; e.g., one can use the average of single-particle energies in the initial and final states. But there is a more serious problem. For those cases in which one or more of the states j_1, j_2, j_3, j_4 is $p_{1/2}$ or $f_{5/2}$, the energy denominator becomes quite small, so that the total correction term becomes large. This is because in the set of single-particle energies we assume, the $g_{9/2}$ orbit is between, and close to, the $p_{1/2}$ and $f_{5/2}$ orbits. An additional problem is that some of the perturbing matrix elements in the numerator are quite large (as discussed above), and this also leads to very large renormalization terms. These large terms make this second-order perturbation approach questionable. We did use this scheme to renormalize the f - p -shell matrix elements of the Kuo-Brown interaction, and then we used the resulting renormalized interaction in a four-shell calculation of the spectrum of ^{42}Ca . The results of this calculation were not in good agreement with the results of the five-shell calculation with the Kuo-Brown interaction, presumably for the reasons we have indicated above. This perturbation method was not pursued any further.²⁰

We return now to our discussion of the Hamiltonian KB' . As Table II shows, the modified Hamiltonian KB' was obtained by changing the Kuo-Brown Hamiltonian KB in these ways. The matrix elements $\langle f_{7/2}^2 \mathcal{J} | V | f_{7/2}^2 \mathcal{J} \rangle$ for $\mathcal{J}=0$ and $\mathcal{J}=2$ were made more attractive by ≈ 0.3 MeV, and all the $\langle f_{7/2} p_{3/2} \mathcal{J} | V | f_{7/2} p_{3/2} \mathcal{J} \rangle$ matrix elements were made more repulsive by ≈ 0.3 MeV. This latter change raises the center of gravity of the $\langle f_{7/2} p_{3/2} \mathcal{J} | V | f_{7/2} p_{3/2} \mathcal{J} \rangle$ interaction from -0.1 MeV to $+0.2$ MeV.

The spectra of ^{42}Ca to ^{50}Ca as calculated with this modified interaction KB' in the vector space f - p are shown in Figs. 10–18. These calculated results are labeled f - p' . For comparison we include in these figures the spectra calculated with

specific: Let j_1 stand for any of the four f - p orbits; let $\langle |V| \rangle_4$ be the new renormalized two-body matrix element to be used in the four-orbit shell-model calculation, and let $\langle |V| \rangle_5$ be the matrix element for the five-shell space as calculated by Kuo-Brown. Then

the f - p model described in Secs. II and III. The results for the f - p model are now labeled f - p (KB), to emphasize that the Kuo-Brown interaction is used in this case, while a *modified* version of the Kuo-Brown interaction is used to obtain the results labeled f - p' . The general rule followed in Figs. 10–18 is to show all theoretical levels up to ≈ 5 MeV, and all observed levels up to the point where the level density becomes relatively high, after which only states having parity $(-)^{(A-40)}$ with reasonable certainty are shown. (Details are given in the captions and in later discussion.) In all the figures except for ^{50}Ca , the position of the lowest-lying observed state with parity $(-)^{(A-40)+1}$ is indicated by a dashed line, and the spin and parity of that state are given on the left side of the spectrum. These states must be predominately core-excited, and therefore they cannot be described by the model used here. In Tables III–XI we present calculated and observed

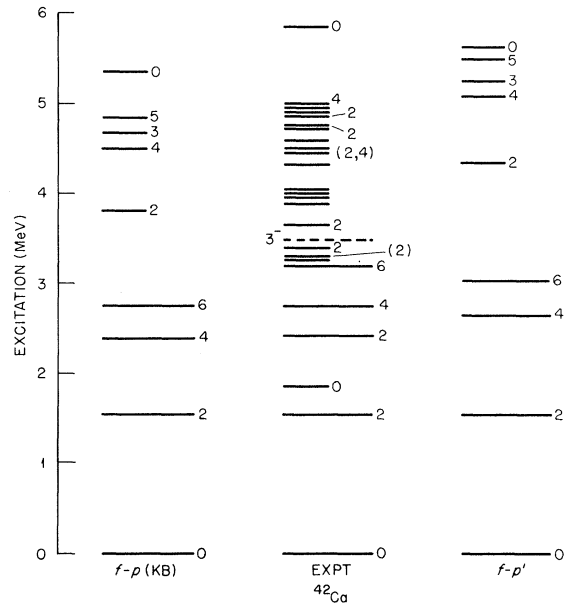


FIG. 10. Calculated and observed excitation spectra in ^{42}Ca . The column labels are explained in Sec. IV. The experimental spectrum is explained in the caption to Fig. 1.

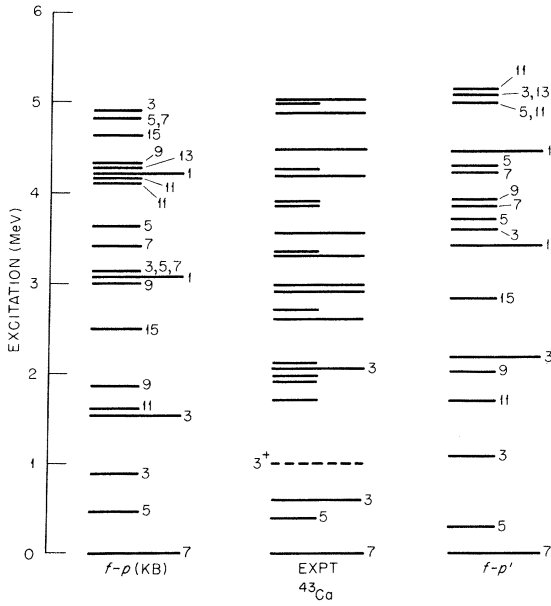


FIG. 11. Calculated and observed excitation spectra in ^{43}Ca . The column labels are explained in Sec. IV. The experimental spectrum is explained in the caption to Fig. 2.

energies, and strengths for single-neutron transfer reaction. For most of the experimentally determined strengths, the orbital angular momentum transfer Δl is known, but not the total angular momentum transfer Δj . To facilitate com-

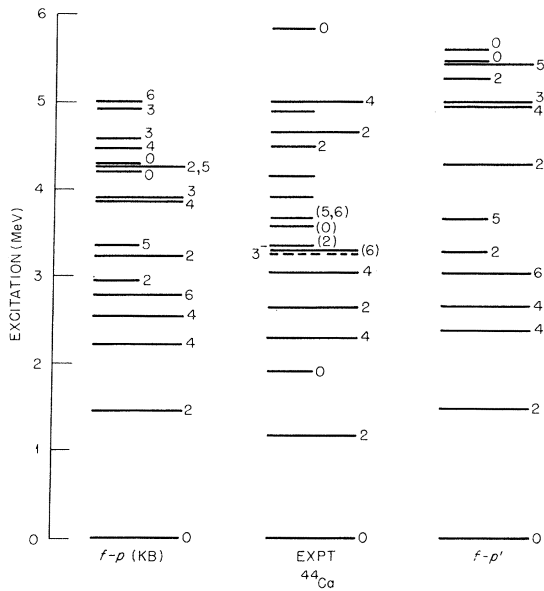


FIG. 12. Calculated and observed excitation spectra in ^{44}Ca . The column labels are explained in Sec. IV. The experimental spectrum is explained in the caption to Fig. 3.

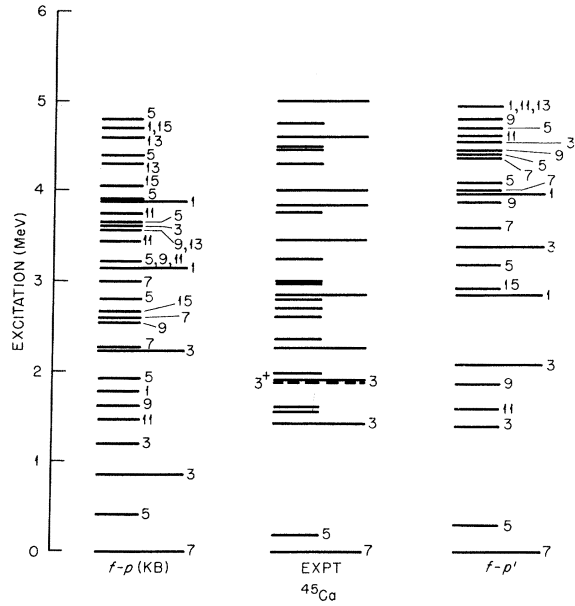


FIG. 13. Calculated and observed excitation spectra in ^{45}Ca . The column labels are explained in Sec. IV. The experimental spectrum is explained in the caption to Fig. 4.

parison with experiment, we list the shell-model strengths in terms of Δl rather than Δj ; i.e., for $\Delta l = 1$ we list the sum $S(p) = S(p_{3/2}) + S(p_{1/2})$, and for $\Delta l = 3$ we list the sum $S(f) = S(f_{5/2}) + S(f_{7/2})$.

We proceed now to a nucleus-by-nucleus dis-

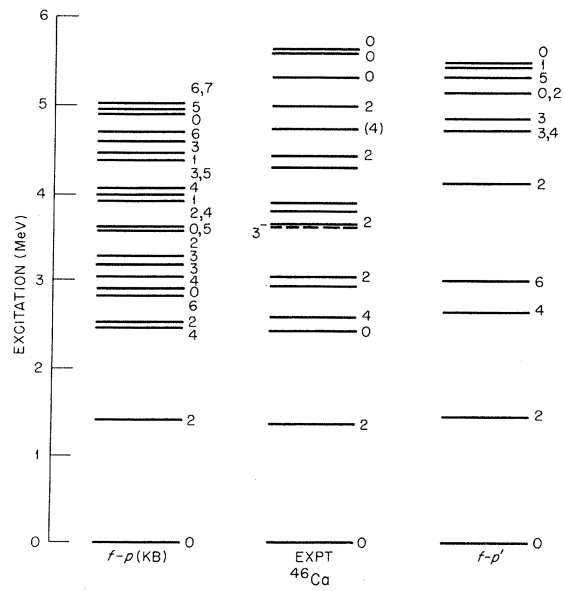


FIG. 14. Calculated and observed excitation spectra in ^{46}Ca . The column labels are explained in Sec. IV. The experimental spectrum is explained in the caption to Fig. 5.

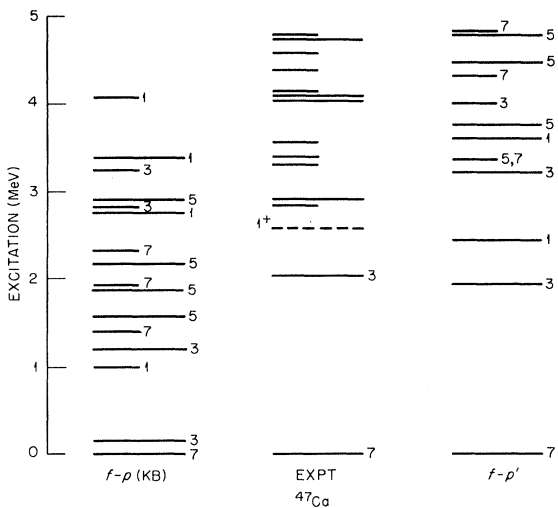


FIG. 15. Calculated and observed excitation spectra in ^{47}Ca . The column labels are explained in Sec. IV. The experimental spectrum is explained in the caption to Fig. 6.

cusson of the $f-p'$ results.

^{42}Ca

The calculated and observed positions of levels in ^{42}Ca are shown in Fig. 10. The experimental spectrum²¹ shows all observed levels below 5 MeV

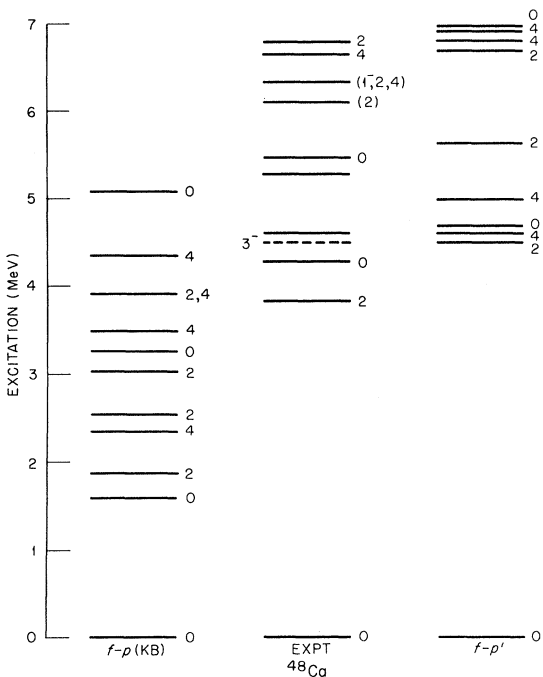


FIG. 16. Calculated and observed excitation spectra in ^{48}Ca . The column labels are explained in Sec. IV. The experimental spectrum is explained in the caption to Fig. 7.

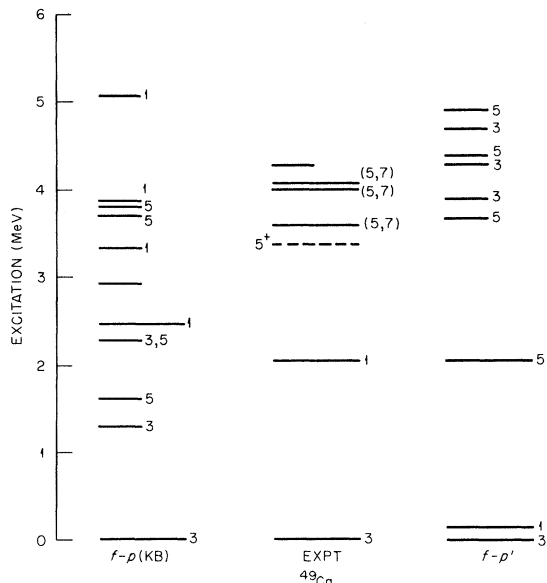


FIG. 17. Calculated and observed excitation spectra in ^{49}Ca . The column labels are explained in Sec. IV. The experimental spectrum is explained in the caption to Fig. 8.

which are not known definitely to be negative-parity levels. There is little difference between the $f-p$ (KB) and $f-p'$ spectra. The major discrepancies with experiment are that the 0^+ state observed at 1.84 MeV, and the 2^+ state observed at 2.42 MeV, are not accounted for by either $f-p$ (KB) or $f-p'$ spectra. This same result has been obtained in all the

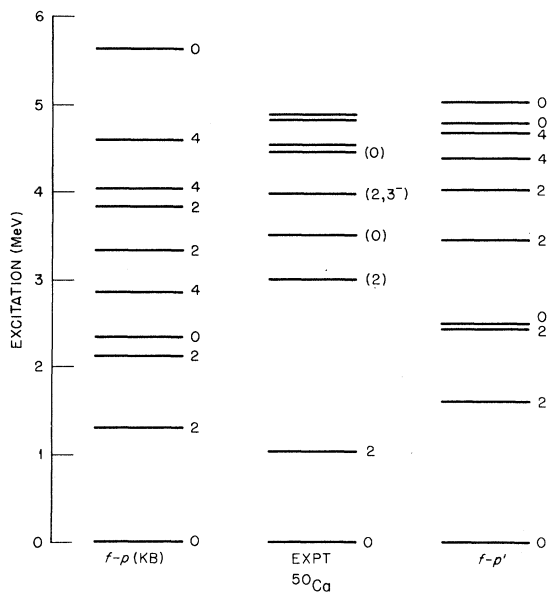


FIG. 18. Calculated and observed excitation spectra in ^{50}Ca . The column labels are explained in Sec. IV. The experimental spectrum is explained in the caption to Fig. 9.

TABLE III. Calculated and observed levels in ^{42}Ca , and spectroscopic factors for $^{43}\text{Ca}(d,t)^{42}\text{Ca}$. The table includes all theoretical levels shown in Fig. 10, plus all observed levels with known spins.

$f-p$ (KB)				$f-p'$				Expt ^a			
E (MeV)	J	Δl	$S(d,t)$	E (MeV)	J	Δl	$S(d,t)$	E (MeV)	J	Δl	$S(d,t)$
0	0	f	0.75	0	0	f	0.75	0	0	f	0.50
1.55	2	f	0.37	1.54	2	f	0.38	1.52	2	f	0.16
2.36	4	f	0.68	2.64	4	f	0.69	1.84	0	f	0.05
2.73	6	f	0.99	3.02	6	f	1.01	2.42	2	f	0.11
3.81	2	$f+p$	0.02+0.01	4.34	2	$f+p$	0.01+0.01	2.75	4	f	0.47
4.50	4	$f+p$	0.01+0.02	5.06	4	$f+p$	0.01+0.02	3.19	6	f	1.00
4.67	3	p	0.01	5.23	3	p	0.02	3.39	2		
4.85	5	$f+p$	0.01+0.01	5.48	5	f	0.02	3.65	2		
5.35	0		<0.01	5.62	0		<0.01	4.45	(2,4)		
								4.75	2		
								4.86	2		
								5.01	4		
								5.85	0		

^aEnergies and spin assignments from Ref. 21, spectroscopic factors from Ref. 22.

$f-p$ -shell calculations which were discussed in the introduction to this paper. (Federman and Talmi⁶ successfully fit these ^{42}Ca levels with *core-excited* configurations.) The observed density of ^{42}Ca states above 3 MeV is much greater than the calculated density. Again, the extra observed states are presumably manifestations of the im-

portance, above 3 MeV, of core-excited configurations not included in our model vector space. In both the $f-p$ (KB) and $f-p'$ spectra, there is a theoretical 0^+ state which roughly matches the energy of the observed 0^+ state at 5.85 MeV.

Yntema²² has studied the reaction $^{43}\text{Ca}(d,t)^{42}\text{Ca}$, and has determined strengths for transfers to

TABLE IV. Calculated and observed energy levels and strengths for states in ^{43}Ca . Here $(2J+1)S_{\uparrow}$ is the strength for $^{42}\text{Ca}(d,p)^{43}\text{Ca}$ (see Ref. 24), and S_{\downarrow} is the strength for $^{44}\text{Ca}(d,t)^{43}\text{Ca}$ (see Ref. 22). An asterisk indicates a spin assignment based on the j dependence of the observed angular distribution. A dotted entry indicates $S \leq 0.01$.

$f-p$ (KB)					$f-p'$					Expt ^a				
E (MeV)	$2J$	Δl	$(2J+1)S_{\uparrow}$	S_{\downarrow}	E (MeV)	$2J$	Δl	$(2J+1)S_{\uparrow}$	S_{\downarrow}	E (MeV)	Δl	$2J$	$(2J+1)S_{\uparrow}$	S_{\downarrow}
0	7	f	6.00	3.60	0	7	f	6.00	3.70	0	f	7	5.50	4.0
0.46	5	f	...	0.02	0.30	5	f	...	0.02	0.37	f	5		≤ 0.15
0.88	3	p	...	0.01	1.07	3	p	0.59	p	3	0.21	0.18
1.52	3	p	3.72	0.15	1.69	11				2.04	p	3	3.00	0.20
1.59	11				2.00	9				2.10	p			0.06
1.79	9				2.16	3	p	3.72	0.08	2.61	p	1*	0.29	
2.48	15				2.82	15				2.62	(f)			0.14
3.02	9				3.41	1	p	1.00	0.02	2.87	p	1*	0.20	
3.06	1	p	0.54	0.04	3.58	3	p	0.08	...	2.94	p	3*	0.24	
3.08	3	p	0.12	0.01	3.69	5	f	3.29	p	3*	0.21	
3.10	5	f	3.83	7	f	0.08	0.02	3.31	p			0.05
3.11	7	f	...	0.03	3.92	9				3.57	p	3*	0.24	
3.36	7	f	4.22	7	f	3.81	(f)			0.16
3.61	5	f	4.30	5	f	3.86	p	1*	0.05	
4.10	11				4.46	1	p	0.88	0.01	4.20	p	(1)*	0.88	
4.16	11				5.00	11				4.24	p			0.12
4.19	13				5.01	5	f	4.46	p			0.36
4.20	1	p	1.34	0.02	5.06	13				4.90	p			0.22
4.30	9				5.08	3	p	5.03	p			0.21
4.64	15				5.09	11								
4.80	17													
4.82	5	f	0.06	...										
4.91	3	p	0.08	...										

^aEnergies and spins from Ref. 24; $(2J+1)S$ values from Ref. 24, and S values from Ref. 22.

TABLE V. Calculated and observed levels in ^{44}Ca , and strengths $(2J_f+1)S/(2J_i+1)$ for $^{43}\text{Ca}(d,p)^{44}\text{Ca}$. A dotted entry indicates strength ≤ 0.01 .

$f-p$ (KB)				$f-p'$				Expt ^a			
E (MeV)	J	Δl	$\frac{(2J_f+1)}{(2J_i+1)}S$	E (MeV)	J	Δl	$\frac{(2J_f+1)}{(2J_i+1)}S$	E (MeV)	J	Δl	$\frac{(2J_f+1)}{(2J_i+1)}S$
0	0	f	0.45	0	0	f	0.46	0	0	f	0.36
1.43	2	f	0.71	1.46	2	f	0.79	1.16	2	f	0.36
2.24	4	f	0.63	2.36	4	f	0.22	1.90	0	f	0.07
2.54	4	f	0.78	2.68	4	f	1.25	2.29	4	f	0.22
2.79	6	f	2.18	3.03	6	f	2.18	2.66	2	f	0.45
2.94	2		0.02	3.29	2		0.01	3.04	4	f	1.46
3.21	2	p	0.44	3.65	5		...	3.30	(6)	f	2.45
3.35	5		...	4.28	2	p	0.46	3.35	(2)		
3.85	4	p	0.88	4.97	4	p	0.85	3.59	(0)		
3.90	3	p	0.71	5.00	3	p	0.71	3.66	(5, 6)		
4.20	0		...	5.27	2		0.03	3.93		p	0.04
4.24	5	p	1.26	5.44	5	p	1.26	4.10		(f)	0.09
4.25	2		0.06	5.47	0		0.01	4.21		p	0.02
4.27	0		...	5.60	0		...	4.49	2	(p)	0.04
4.49	4		...					4.66	2	p	0.28
4.58	3		...					4.91		p	0.12
4.92	3		...					4.99		p	0.05
5.01	6		...					5.02	4	p	0.25

^a From Ref. 26.

TABLE VI. Calculated and observed energies in ^{45}Ca ; strengths $(2J+1)S_{\dagger}$ for $^{44}\text{Ca}(d,p)^{45}\text{Ca}$; and strengths S_{\dagger} for $^{46}\text{Ca}(p,d)^{45}\text{Ca}$. An asterisk indicates a j assignment based on the j dependence of angular distribution in (d,p) reaction. A dotted entry indicates $(2J+1)S < 0.01$.

$f-p$ (KB)					$f-p'$					Expt ^a				
E (MeV)	$2J$	Δl	$(2J+1)S_{\dagger}$	S_{\dagger}	E (MeV)	$2J$	Δl	$(2J+1)S_{\dagger}$	S_{\dagger}	E (MeV)	$2J$	Δl	$(2J+1)S_{\dagger}$	S_{\dagger}
0	7	f	4.04	5.22	0	7	f	4.00	5.57	0	7	f	3.36	6.0
0.41	5	f	...	0.02	0.30	5	f	...	0.02	0.18	5			
0.86	3	p	3.32	0.26	1.37	3	p	...	0.01	1.43	3	p	0.47	
1.21	3	p	0.12	0.04	1.59	11				1.56				
1.47	11				1.87	9				1.58				
1.61	9				2.08	3	p	3.38	0.07	1.90	3	p	2.56	
1.79	1	p	0.14	...	2.85	1	p	0.68	0.01	1.97				
1.93	5	f	2.65	15				2.25	1*	p	0.36	
2.22	3	p	0.24	0.02	3.18	5	f	2.36				
2.25	7	f	0.16	0.09	3.37	3	p	0.24	0.01	2.60				
2.56	9				3.58	7	f	0.08	0.04	2.68				
2.58	7	f	...	0.05	3.88	9				2.77				
2.65	15				3.97	1	p	1.00	0.02	2.85	3*	p	0.46	
2.80	5	f	4.00	7	f	...	0.01	2.95				
2.98	7	f	4.08	5	f	2.97				
3.14	1	p	0.48	0.01						3.25	1*	p	0.12	
3.87	1	p	1.10	0.03						3.44	1*	p	0.79	
										3.79		(p)	0.16	
										3.85	3*		0.26	
										3.99		p	0.65	
										4.46		p	0.09	
										4.62		p	0.45	
										5.00		p	0.50	

^a Energies, spins, and (d,p) strengths $(2J+1)S$ from Ref. 30; (p,d) strengths S from Ref. 22.

TABLE VII. Calculated and observed levels in ^{46}Ca .

$f-p$ (KB)		$f-p'$		Expt ^a	
E	J	E	J	E	J
(MeV)		(MeV)		(MeV)	
0	0	0	0	0	0
1.39	2	1.44	2	1.35	2
2.45	4	2.63	4	2.43	0
2.51	2	3.06	6	2.57	4
2.83	6	4.12	2	2.98	
2.92	0	4.74	4	3.02	2
3.03	4	5.13	0	3.64	2
3.55	2	5.12	2	3.78	
3.60	0	5.49	0	3.86	
3.89	2			4.28	
3.86	4			4.43	2
4.05	4			4.74	(4)
4.68	6			4.98	(2)
4.90	0			4.32	0
5.03	6			5.60	0
				5.63	0

^a From Ref. 23.

some of the low-lying states in ^{42}Ca . The shell-model and empirical S factors for this reaction are shown in Table III. The calculated strength for the ground-state transition, 0.75, is not in good agreement with the experimental value, 0.50. However, this S factor should be the same as the S factor determined from the ground-state to ground-state transition in $^{42}\text{Ca}(d,p)^{43}\text{Ca}$; and the S factor empirically determined from the (d,p) data²⁴ is 0.75, in good agreement with the calculated values shown in Table III. In the $^{43}\text{Ca}(d,t)^{42}\text{Ca}$

experiment there is significant strength to both low-lying 2^+ states. Suppose we sum these two observed strengths to the 2^+ states, and consider this sum as the empirically determined result to be compared with shell-model results. Then we find that the relative values of shell-model strengths for the lowest 0^+ , 2^+ , and 4^+ states are in excellent agreement with the corresponding *relative* values from experiment. Thus, the first $J=0^+$, 2^+ , 4^+ , and 6^+ states of the model can be correlated with experimental levels. For excitations above these levels, the model space is too restricted to account for the observed level density.

 ^{43}Ca

The calculated and observed²⁴ spectra of ^{43}Ca are shown in Fig. 11. The experimental spectrum in Fig. 11 includes all known levels below 2.0 MeV which are not assigned definite positive parity. Between 2.0 and 5.0 MeV, there are 66 observed levels which are possible negative-parity states. But above 2 MeV in the experimental spectrum of Fig. 11, we show only those levels which are definitely observed to be populated with $l=1$ or $l=3$ transitions in the reaction $^{42}\text{Ca}(d,p)^{43}\text{Ca}$. Thus between 2 and 5 MeV the number of observed levels is about four times the number shown in column EXPT of Fig. 11. There is again little difference between the two calculated spectra, except for the slight expansion of the $f-p'$ spacings over the $f-p$ (KB) spacings. Information about S factors is given both in Table IV and in Fig. 10. In Table IV the

TABLE VIII. Calculated and observed energy levels of ^{47}Ca , and calculated and observed strengths for (d,p) and (p,d) reactions to levels in ^{47}Ca . A dotted entry indicates $(2J+1)S_{\uparrow} < 0.01$ or $S_{\downarrow} < 0.01$. An entry n.c. means the value was not calculated.

$f-p$ (KB)					$f-p'$					Expt ^a				
E	$2J$	Δl	$(2J+1)S_{\uparrow}$	S_{\downarrow}	E	$2J$	Δl	$(2J+1)S_{\uparrow}$	S_{\downarrow}	E	$2J$	Δl	$(2J+1)S_{\uparrow}$	S_{\downarrow}
(MeV)					(MeV)					(MeV)				
0	7	f	2.16	6.38	0	7	f	2.08	7.50	0	7	f	2.20	6.5
0.15	3	p	3.08	0.51	1.94	3	p	3.20	0.03	2.01	3	p	3.30	0.03-0.05
1.00	1	p	0.10	...	2.45	1	p	0.94	0.01	2.86		p	0.08	0.05
1.20	3	p	0.44	0.15	3.24	3	p	0.48	0.03	2.88	(1)	p	0.49	
1.38	7	f	0.16	0.14	3.36	5	f	0.08	n.c.	3.30				0.04-0.08
1.58	5	f	...	n.c.	3.37	7	f	...	0.02	3.43		p		0.02-0.08
1.88	5	f	0.01	n.c.	3.64	1	p	0.80	0.02	3.57				
1.92	7	f	0.08	0.30	3.77	5	f	0.01	n.c.	4.01	(3)	p	0.52	
2.18	5	f	...	n.c.	4.04	3	p	0.12	0.01	4.05	(1)	p	0.99	0.50-0.10
2.33	7	f	...	0.07	4.34	7	f	...	0.05	4.40		p	0.05	0.04-0.08
2.76	1	p	0.90	0.04	4.50	5	f	0.26	n.c.	4.59		p		0.09
2.79	3	p	4.82	5	f	0.14	n.c.	4.78		p	0.79	
2.88	5	f	0.01	n.c.	4.85	7	f	0.08	...	4.80		p	0.26	
3.25	3	p	4.85	7	f	0.08						
3.38	1	p	0.64	0.02										
4.06	1	p										

^aThe (d,p) strengths are from Ref. 31; the (p,d) strengths from Ref. 32.

TABLE IX. Calculated and observed energy levels of ^{48}Ca .

$f-p$		$f-p'$		E	
E	J	E	J	E	J
(MeV)		(MeV)		(MeV)	
0	0	0	0	0	0
1.57	0	4.49	2	3.83	2
1.87	2	4.61	4	4.28	0
2.35	4	4.68	0	4.60	
2.52	2	4.99	4	5.30	
3.02	2	5.64	2	5.46	0
3.24	0	6.69	2	6.11	(2)
3.48	4	6.83	4	6.35	(1 ⁻ , 2, 4)
3.91	2	6.92	4	6.65	4
3.93	4	6.97	0	6.80	2
4.35	4				
5.09	0				

^aFrom Refs. 21 and 23.

calculated and observed energies of ^{48}Ca are tabulated, together with calculated and experimentally determined strengths for the $^{42}\text{Ca}(d,p)^{43}\text{Ca}$ reaction²⁴ and the $^{44}\text{Ca}(d,t)^{43}\text{Ca}$ reaction.²² In Fig. 11, levels for which $(2J_f + 1)S \geq 0.20$ are indicated by long lines. The calculated strengths for the ground-state transitions are consistent with experiment. The position of the first calculated $\frac{3}{2}^-$ state is somewhat too high. Table IV shows that the (d,p) strength to this state is too small compared with experiment. The experimental data indicate more mixing of (d,p) strength between the first two $\frac{3}{2}^-$ states than is given by calculations. The calculations put most of the $p_{3/2}$ strength in the state near 2.0 MeV.

Above 2.0 MeV in ^{43}Ca , there are nine observed states with $(2J+1)S \geq 0.20$. In each of the calculated spectra, there are only two states calculated to have $(2J+1)S \geq 0.20$, and both these states have $J^\pi = \frac{1}{2}^-$. There is no clear-cut correlation between the various theoretical and experimental states above 2.0 MeV. There is evidence of a j dependence in the angular distribution of the emitted protons in the (d,p) reaction here. The j -dependent effects are not well understood theoretically, and spin assignments made solely on the basis of j dependence must still be considered uncertain. In Table IV, the spins implied by j dependence alone are indicated by asterisks. If these assignments are correct, a significant part of the $p_{3/2}$ strength ($\approx 20\%$) is observed between 2.9 and 3.6 MeV; but in the shell models almost all the $p_{3/2}$ strength is in the single state at ≈ 2.0 MeV. In the observed spectrum, the $p_{1/2}$ strength appears to be spread over a number of states; but in each of the calculated spectra, almost the entire $p_{1/2}$ strength (≈ 1.9 out of the total 2.0) is in

two states.

There is a proposed $\frac{1}{2}^-$ state observed at 4.2 MeV with a strength $(2J+1)S = 0.88$. This is close to the calculated $\frac{1}{2}^-$ state at 4.46 MeV, which has the same strength. However, if the assumed $\frac{1}{2}^-$ states in the experimental spectrum are correct, then the observed $\frac{1}{2}^-$ states below 4.0 MeV do not have enough strength to match the strength to the theoretical state at 3.41 MeV.

The total observed $l=1$ strength for $p_{1/2}$ and $p_{3/2}$ transitions to states below 5.03 MeV is 5.98, compared to the theoretical maximum of 6, from the shell-model sum rule. The calculated total strength below 5.08 MeV is 5.76. If we again assume the spin assignments inferred from j dependence, then the center of gravity of the $p_{3/2}$ strength, defined as

$$\sum_i (2J+1)S_i E_i / \sum_i (2J+1)S_i,$$

is 2.2 MeV from experimental states, compared to 2.3 MeV calculated from the $f-p'$ model. For the $p_{1/2}$ strength, the center of gravity is 4.0 from experiment versus 3.9 from the $f-p'$ model. The observed and calculated $l=3$ strengths around 5.0 MeV are too small to allow us to draw any meaningful conclusions.

It would obviously be very useful to have more definite spin assignments for the $\frac{1}{2}^-$ and $\frac{3}{2}^-$ states in the odd calcium isotopes. Such assignments may become available as the stripping experiments are repeated with polarized deuterons.²⁵ Since there are so many uncertainties in the analysis of experimental data on $p_{1/2}$ strengths, it does not seem worthwhile now to attempt to alter the shell model (i.e., by shifting the $p_{1/2}$ s.p.e. or changing the $f_{7/2}-p_{1/2}$ matrix elements) to obtain better agreement with these empirical strengths. As was pointed out above, the calculations we have made are expected to be more accurate for the states dominated by $f_{7/2}-p_{3/2}$ configurations than for states in which there is significant occupation of $p_{1/2}$ or $f_{5/2}$ orbits. In particular, the calculated positions of the $p_{1/2}$ or $f_{5/2}$ strengths, relative to the $f_{7/2}-p_{3/2}$ states, are not expected to be too accurate.

^{44}Ca

The calculated and observed spectra of ^{44}Ca are shown in Fig. 12. In the experimental spectrum, all known positive-parity levels up to 3.0 MeV are shown. Above 3 MeV, all levels are shown which either have tentative spin assignments based on the $^{42}\text{Ca}(t,p)^{44}\text{Ca}$ reaction,²³ or which are known to be populated with $l=1$ or $l=3$ strength in the $^{43}\text{Ca}(d,p)^{44}\text{Ca}$ reaction.²⁶ Levels

populated with strengths $[(2J_f + 1)/(2J_i + 1)]S \geq 0.2$ are drawn with longer lines. There are 28 levels known in ^{44}Ca below 5 MeV which are not definitely negative-parity states. Of these, 16 are seen in the (t, p) experiment.

A comparison of the two calculated spectra shows that the $f-p$ (KB) and $f-p'$ results for the low-lying $f_{7/2}$ states are similar. For states above 3.0 MeV, the $f-p'$ spectrum is expanded and generally higher than the $f-p$ (KB) spectrum. For states shown in the observed spectrum up to 3.5 MeV, the agreement between theory and experiment is quite good, with two notable exceptions. Neither of the calculated spectra shows a reasonable analog to the observed 0^+ state at 1.90 MeV; and also, there seems to be an extra 2^+ state in the experimental spectrum. We have made a number of other calcium calculations²⁷ (which we shall not discuss in detail here); in these we used a variety of different phenomenological interactions, all adjusted to fit selected sets of observed levels. The interactions included a modified surface delta interaction,²⁸ a potential parametrized in terms of radial integral parameters,²⁹ and interactions for which we used some of the Kuo-Brown interaction matrix elements, while treating other matrix elements as adjustable parameters. In none of these calculations did a second 0^+ state in ^{44}Ca appear close to the observed 1.90-MeV state. It appears to us that, in order to account for the position of this second 0^+ state, it is necessary to include in the basis-vector space some core-excited configurations.

Table V lists calculated and observed energies for ^{44}Ca , and calculated and observed strengths for the reaction $^{43}\text{Ca}(d, p)^{44}\text{Ca}$. There is a significant difference between the $f-p$ (KB) and $f-p'$ strengths. The difference is in the distribution of $l=3$ strength between the first two 4^+ states in ^{44}Ca . The calculated energies of these states are not very different in the two models. However, in the $f-p$ (KB) calculation, the strength is almost equally distributed between the two 4^+ states, while in the $f-p'$ calculation, the second state has six times the strength of the first state. The strengths calculated with the $f-p'$ model are in excellent agreement with the strengths extracted from experiment. In both models there is a strong transition to the first 2^+ state, and no appreciable strength to the second 2^+ state. The calculated strength to the first 2^+ state (0.71 in the $f-p$ (KB) model and 0.79 in the $f-p'$ model) is very close to the sum of experimentally determined strengths to the first two observed 2^+ states. A plausible interpretation here is that the experimental spectrum includes an *extra* 2^+ state

(having a structure similar to the 0^+ state observed at 1.90 MeV), and that this extra 2^+ state mixes with the $f-p$ -shell state. In going from the $f-p$ (KB) model to the $f-p'$ model, the first two excited 0^+ states move up together by more than an MeV, and in the $f-p'$ model they occur at about the same energy as the observed 0^+ state at 5.86 MeV. In all the calculations we have made, these two 0^+ states remain fairly close together; they never appear at a large enough separation so that they would account for the pair of observed states at 3.59 MeV and at 5.86 MeV. In the $f-p'$ calculation there are four ^{44}Ca states with a total $l=1$ strength of 3.28. Three of these $l=1$ states lie below 5.0 MeV. As we see from Table V, below 5.02 MeV the total observed $l=1$ strength is 0.80. Between 5.1 and 6.2 MeV, the (d, p) experiment shows definite $l=1$ transitions to 11 states, with a total strength of 3.28. Thus in ^{44}Ca the $f-p'$ calculation seems to put the $l=1$ strength too low by about 1 MeV.

In general, both models account for most of the ^{44}Ca levels up to 3.5 MeV. We reiterate that there are a number of possible even-parity levels observed above 3.5 MeV which are not shown either in Fig. 11 or in Table V, so that here, as in all the isotopes we have treated, the density of observed states is much greater than the calculated density at energies above the position of the higher $f_{7/2}$ states.

^{45}Ca

The calculated and observed spectra for ^{45}Ca are shown in Fig. 13 and tabulated in Table VI. Table VI also shows the calculated and observed strengths for the reaction $^{44}\text{Ca}(d, p)^{45}\text{Ca}$,³⁰ and the reaction $^{46}\text{Ca}(d, t)^{45}\text{Ca}$.²²

The experimental spectrum in Fig. 13 shows all possibly negative-parity states below 3.0 MeV, and all states between 3.0 and 5.0 MeV which are populated with $l=1$ or $l=3$ transitions. There are 20 possibly negative-parity states omitted in the experimental spectrum between 3.0 and 5.0 MeV. The difference between the $f-p$ (KB) and $f-p'$ results is more striking here than for the lighter isotopes, and here the $f-p'$ results are significantly better than the $f-p$ (KB) results. For levels in the first 2.0 MeV, the agreement between the $f-p'$ spectrum and the observed spectrum is good. There is an observed transition to the first $\frac{3}{2}^-$ state, at 1.43 MeV; the strength $(2J_f + 1)S$ is 0.47. In the $f-p$ (KB) model, most of the total strength is to the first $\frac{3}{2}^-$ state, at 0.86 MeV. In the $f-p'$ model, most of the $p_{3/2}$ strength is to the second $\frac{3}{2}^-$ state; this result is in significantly better agreement with experiment. In Table VI

we have again used an asterisk to indicate tentative spin assignments based on the j dependence of the angular distribution in the (d, p) experiment. As in ^{43}Ca , there is no clear-cut correlation between calculation and experiment for $\frac{1}{2}^-$ states and higher $\frac{3}{2}^-$ states. However, for the states shown in Table VI, the f - p' model yields a centroid for the $p_{3/2}$ strength at 2.2 MeV, in good agreement with the observed centroid at 2.1 MeV. The $p_{1/2}$ centroid of strength calculated from the f - p' model is at 3.5 MeV, while the experimentally observed centroid is at 3.9 MeV. Here again, firm spin assignments for the observed states between 2.0 and 5.0 MeV would be very helpful. We note that, as for the lighter isotopes, our shell models give only about half the observed density of states between 2 and 5 MeV.

^{46}Ca

The calculated and observed spectra of ^{46}Ca are shown in Fig. 14, and tabulated in Table VII. The observed levels were determined from experiments involving the $^{44}\text{Ca}(t, p)^{46}\text{Ca}$ reaction.²³ Figure 14 shows all of the levels observed below 5.0 MeV, and also the three 0^+ states observed between 5.0 and 6.0 MeV. Recall that in the case of ^{44}Ca , where data on both the $^{43}\text{Ca}(d, p)^{44}\text{Ca}$ and $^{42}\text{Ca}(t, p)^{44}\text{Ca}$ reactions were available, there were roughly twice as many levels observed below 5 MeV with the (d, p) reaction as with the (t, p) reaction. This suggests that in ^{46}Ca , where only (t, p) results are available, the density of levels below 5 MeV may be at least twice as high as shown in Fig. 13. There is a striking difference in ^{46}Ca between the f - p (KB) calculation and the f - p' calculation. In particular, between 3 and 5 MeV the f - p (KB) model gives a much higher density of levels than is given by the f - p' model. The $f_{7/2}$ states are well accounted for by both models. The f - p (KB) model gives an excited 0^+ state not too far above the observed 0^+ state at 2.42 MeV. However, the calculated position of this second 0^+ state is very sensitive to the relative position of the $p_{3/2}$ center of gravity $C_{7/2, 3/2}$; this is evidenced by the behavior of the excited 0^+ states when the $f_{7/2}$ - $p_{3/2}$ interaction is altered to give the f - p' model. In the f - p' model, the two excited 0^+ states are close in energy to the set of three 0^+ states observed between 5.0 and 6.0 MeV.

^{47}Ca

The observed and calculated spectra of ^{47}Ca are shown in Fig. 15. The energy levels are tabulated in Table VIII, together with the observed and calculated strengths for the reaction $^{46}\text{Ca}(d, p)^{47}\text{Ca}$,³¹

and the reaction $^{48}\text{Ca}(p, d)^{47}\text{Ca}$.³² Figure 14 and Table VIII show a significant difference between the f - p (KB) and f - p' results for ^{47}Ca . There is little resemblance between the spectrum calculated with the f - p (KB) model and the observed spectrum; but there is a significant improvement in the f - p' calculation, which yields a $p_{3/2}$ strength raised by almost 2 MeV compared to that of the f - p (KB) calculation. The observed strengths to the lowest two excited states imply that these states are relatively pure single-particle states, and this pattern is reproduced by the f - p' calculation. Again, there is little experimental information on the spins of the remaining states in ^{47}Ca . If the tentative $\frac{1}{2}^-$ assignments to the observed states at 2.88 and 4.05 MeV are correct, then the total observed strength to these two states, 1.48, compares reasonably well with the summed strength 1.70 that the f - p' model yields for its $\frac{1}{2}^-$ states at 2.45 and 3.64 MeV. However, the centroid of this calculated strength is 0.7 MeV below the centroid of the observed strength.

There is a ^{47}Ca state at 4.78 MeV which is observed to be populated by an $l=3$ transition in the (d, p) reaction, with a strength $(2J+1)S=0.78$. In the f - p' model, there is a $\frac{5}{2}^-$ state at 4.50 and another one at 4.82 MeV. The total calculated $l=3$ (d, p) strength to these two states is 0.40. If one correlates these two calculated states with the observed state, then the energies of the states are in good agreement, but the calculated strength is too small by a factor of 2. We shall discuss the sensitivity of the $\frac{1}{2}^-$ and $\frac{5}{2}^-$ states to the interaction at the end of this section.

^{48}Ca

The calculated and observed energy levels of ^{48}Ca are shown in Fig. 16, and they are tabulated in Table IX. The observed spectrum has been determined from experimental studies of the $^{46}\text{Ca}(t, p)^{48}\text{Ca}$ reaction²³ and $^{48}\text{Ca}(\alpha, \alpha')^{48}\text{Ca}$ reaction.²¹ The experimental levels at 4.61, 5.30, and 6.11 MeV were not observed in the (t, p) reaction. Since most of the observed levels lie above 5.0 MeV, we have extended the energy scale to 7.0 MeV for this isotope.

There is obviously a discrepancy between the f - p (KB)-model spectrum and the observed spectrum. In particular, in the f - p (KB) spectrum the excited states all appear to be too low by about 2.5 MeV. This discrepancy is significantly reduced in the f - p' -model calculation, for the 300-keV change in the $f_{7/2}$ - $p_{3/2}$ interaction raises the excited states in the calculated spectrum by more than 2 MeV. The first two excited states in ^{48}Ca apparently can be accounted for by this

f - p' model. Most of the remaining states shown are insensitive to the matrix elements involving any $p_{1/2}$ or $f_{5/2}$ particles. Of the levels in Fig. 16, only the second, third, and fourth 4^+ states in the f - p' model are dominated by configurations with particles in the $p_{1/2}$ or $f_{5/2}$ orbits. The third 2^+ state has about 50% of its wave function in the $f_{7/2}$ - $p_{3/2}$ space; and in all the rest of the states shown, components in the $f_{7/2}$ - $p_{3/2}$ space comprise 65% or more of the wave function. Thus, the relative spacings of most of the higher levels in Fig. 16 will be sensitive to matrix elements involving the $f_{7/2}$ and $p_{3/2}$ orbits. With the exception of the third f - p' 0^+ state, all the f - p' model levels have possible observed analogs within about 500 keV. A comparison of the f - p' model and experiment thus suggests the existence of a 0^+ state in the observed spectrum between 4.0 and 6.0 MeV which contains large admixtures of configurations outside the f - p shell. Considering the known shortcomings of the model, this "prediction" is highly speculative. However, it is consistent with an analysis of the $^{46}\text{Ca}(t,p)^{48}\text{Ca}$ reaction by Kolltveit.³³

⁴⁹Ca

The calculated and experimental spectra for ⁴⁹Ca are shown in Fig. 17. All observed states below 5.0 MeV which are not assigned positive parity are shown in the figure. For this nucleus, only states with $J^\pi = \frac{1}{2}^-$, $\frac{3}{2}^-$, and $\frac{5}{2}^-$ were calculated. The analogous calculations for the other J values are prohibitively large. Table X shows the calculated and observed energies, and the calculated and empirical strengths for the $^{48}\text{Ca}(d,p)^{49}\text{Ca}$ reaction.³⁴ In this case neither the f - p or the f - p'

calculations are in agreement with experiment. In the simplest picture, the spectrum of ⁴⁹Ca would consist of one $\frac{3}{2}^-$ state, one $\frac{1}{2}^-$, and one $\frac{5}{2}^-$ state, each made up of a single particle outside an inert ⁴⁸Ca core. Thus, in our nine-particle model, the spectrum is extremely sensitive to the position of the single-particle strengths for orbits $p_{3/2}$, $p_{1/2}$, and $f_{5/2}$. In our f - p' model of ⁴⁹Ca, the $\frac{1}{2}^-$ and $\frac{5}{2}^-$ strengths are too low by about 2 MeV. In this f - p' model the $\frac{3}{2}^-$ ground state of ⁴⁹Ca is essentially a single-particle state, in agreement with experiment.

⁵⁰Ca

The calculated and observed²³ spectra for ⁵⁰Ca are shown in Fig. 18, and the energies are listed in Table XI. All calculated and observed levels below 5.0 MeV are illustrated and tabulated. There is not a very large difference between the two calculated spectra. Recall that in the lighter isotopes there were low-lying states with essentially no $p_{3/2}$ -particle admixtures, and there were other levels dominated by configurations with one $p_{3/2}$ particle. A change in the $f_{7/2}$ - $p_{3/2}$ interaction would alter the relative position of these two classes of states. In ⁵⁰Ca there is no such distinction between the various low-lying states. There are no pure- $f_{7/2}$ states, and most of the states contain significant admixtures of configurations with at least two $p_{3/2}$ particles in them. Thus the low-lying spectrum in ⁵⁰Ca is sensitive to parts of the interaction to which the low-lying spectra of the lighter isotopes are insensitive. Small errors in the one- and two-body interaction matrix elements can lead to large discrepancies in the ten-particle spectrum of ⁵⁰Ca. Furthermore, the neglect of

TABLE X. Calculated and observed energy levels of ⁴⁹Ca, and strengths for the reaction $^{48}\text{Ca}(d,p)^{49}\text{Ca}$ reaction. A dotted entry indicates $S_\dagger \leq 0.01$.

f - p				f - p'				Expt ^a			
E (MeV)	$2J$	Δl	$(2J+1)S_\dagger$	E (MeV)	$2J$	Δl	$(2J+1)S_\dagger$	E (MeV)	$2J$	Δl	$(2J+1)S_\dagger$
0	3	p	3.04	0	3	p	3.72	0	3	p	4.12
1.29	3	p	0.08	0.14	1	p	1.76	2.03	1	p	2.66
1.60	5	f	...	2.05	5	f	5.16	3.60	(5)	f	0.66
2.27	3	p	...	3.67	5	f	...	4.01	5	f	4.32
2.29	5	f	...	3.89	3	p	...	4.08	(5)	f	0.36
2.46	1	p	1.50	4.29	3	p	0.04	4.28			...
2.94	3	p	...	4.38	5	f	0.06				
3.32	1	p	0.10	4.69	3	p	...				
3.70	5	f	...	4.92	5	f	...				
3.79	5	f	...								
3.85	1	p	0.06								
5.06	1	p	...								

^aFrom Ref. 34.

TABLE XI. Calculated and observed (see Ref. 23) energy levels of ^{50}Ca .

$f-p$		$f-p'$		Expt ^a	
E	J	E	J	E	J
(MeV)		(MeV)		(MeV)	
0	0	0	0	0	0
1.30	2	1.60	2	1.03	2
2.11	2	2.45	2	3.00	(2)
2.33	0	2.49	0	3.52	(0)
2.86	4	3.47	2	3.99	(2 ⁺ , 3 ⁻)
3.31	2	4.01	2	4.47	(0)
3.82	2	4.68	4	4.52	
4.04	4	5.19	4	4.83	
4.60	4	4.80	0	4.88	
5.62	0	5.05	0	5.04	

^aFrom Ref. 23.

many-body terms in the effective Hamiltonian could be important when ten active nucleons are present. Thus it is not too surprising that there is only qualitative agreement between calculation and observation for ^{50}Ca .

The above discussion for ^{42}Ca - ^{50}Ca shows that with relatively small changes of the Kuo-Brown interaction, the observed energy levels and strength distributions of the $f_{7/2}$ states and of the dominant $p_{3/2}$ single-particle strengths in ^{42}Ca to ^{50}Ca can be quite well reproduced. Most of the observed levels with firm spin identification are $f_{7/2}$ states. Thus by searching to find an optimum set of values for the $f_{7/2}$ matrix elements, a large measure of agreement with experiment is assured. However, there are enough observed features besides the $f_{7/2}$ states to indicate that in the heavier Ca isotopes, the position of the $p_{3/2}$ single-particle strength as calculated from the Kuo-Brown interaction must be raised in some manner - e.g., by raising the $p_{3/2}$ s.p.e. as the mass increases, or by raising the center of gravity of the $f_{7/2}$ - $p_{3/2}$ two-body interaction by about 300 keV. When the Kuo-Brown interaction is altered in the latter way, the centroid of single-particle $p_{3/2}$ strength is put at roughly the right excitation in all the calcium isotopes from ^{44}Ca to ^{49}Ca . With this modified interaction, the comparisons of calculation with experiment suggest that the first excited 0^+ states in $^{42,44,46}\text{Ca}$ cannot be accounted for by $f-p$ -shell configurations. This conclusion is consistent with those from all the calculations of the calcium isotopes discussed in the Introduction, with the exception of the conclusion of Federman and Talmi.⁶ Federman and Talmi concluded that the first-excited 0^+ state in ^{44}Ca could be adequately described in terms of configurations having active $f_{7/2}$ and $p_{3/2}$ particles only. They varied 13 two-body matrix elements to get a least-

squares fit to 30 levels in ^{42}Ca to ^{50}Ca . Of these 30 levels, only 10 are not reasonably well described by a pure- $f_{7/2}$ calculation. Thus, 20 of the levels were essentially accounted for by the 4 pure- $f_{7/2}$ two-body matrix elements. This left 9 matrix elements free to fit the remaining 10 levels, including the excited 0^+ state in ^{44}Ca .

It is interesting to compare the various interactions which have been used in calculations of the calcium isotopes. In Table II, matrix elements involving the $f_{7/2}$ and $p_{3/2}$ orbits are given for the Engeland-Osnes interaction, the Federman-Talmi interaction, the Kuo-Brown interaction, and the modified Kuo-Brown interaction used in our $f-p'$ calculation. The pure- $f_{7/2}$ matrix elements are quite similar in all four interactions. The largest difference for these four matrix elements is for the $J=0$ matrix elements. We see that as the model space is increased in size, this matrix element decreases in size. Aside from the pure- $f_{7/2}$ matrix elements, there is little similarity among the interactions. In general, the Federman-Talmi interaction is stronger than the Kuo-Brown interaction. In making any comparison of these interactions, one should remember that each interaction was meant to be used in a different model space.

For the $J^\pi = \frac{1}{2}^-$ and $\frac{5}{2}^-$ states, the results of our $f-p$ (KB) and $f-p'$ calculations are not conclusive. The inadequacy of our basis-vector spaces for these states discourages any extensive investigation of the interaction needed to reproduce experimental data on these states. However, we did make one calculation in which the Hamiltonian used in the $f-p'$ calculations was further modified, in an attempt to raise the centroid of strength for states formed via $p_{1/2}$ and $f_{5/2}$ transfer. The modification was that we added +250 keV to all the diagonal matrix elements of the form $\langle f_{7/2} p_{1/2} J | V | f_{7/2} p_{1/2} J \rangle$ and $\langle f_{7/2} f_{5/2} J | V | f_{7/2} f_{5/2} J \rangle$. The effect of this change is to raise the centers of gravity of the interaction of $p_{1/2}$ and $f_{5/2}$ particles with $f_{7/2}$ particles. Let us use the abbreviation $f-p''$ in referring to calculations with this further-modified Hamiltonian. The results of the $f-p''$ calculation may be summarized as follows:

- (1.) For the low-lying spectra of ^{42}Ca to ^{46}Ca , there are no significant differences between the $f-p'$ and $f-p''$ results.
- (2.) For ^{47}Ca , the $f-p''$ calculation moves the first $\frac{1}{2}^-$ state 400 keV above its position in the $f-p'$ calculation, and it moves the second $\frac{1}{2}^-$ state 900 keV higher. Both these changes improve the agreement of the model spectrum with the observed spectrum.
- (3.) For ^{48}Ca , the $f-p''$ calculation moves the second 0^+ and 2^+ states 300 keV above their analogs

in the f - p' spectrum. It is not clear whether these changes improve the agreement of the model spectrum with the observed spectrum. The positions of the other low-lying levels are unchanged.

(4.) For ^{49}Ca , the first $\frac{1}{2}^-$ state in the f - p'' model is at 1.84 MeV; this is within 200 keV of the observed $\frac{1}{2}^-$ state at 2.03 MeV. Also, the first two $\frac{5}{2}^-$ states in the f - p'' model are degenerate at 3.74 MeV. This latter result is consistent with experimental data, for there are three experimentally observed states between 3.6 and 4.1 MeV which are populated with $l=3$ transfers in the $^{48}\text{Ca}(d,p)^{49}\text{Ca}$ reaction.³⁴

(5.) In ^{50}Ca , the second 0^+ state is very sensitive to the 250-keV changes in the centers of gravity of the $f_{7/2}$ - $p_{1/2}$ and $f_{7/2}$ - $f_{5/2}$ interactions which were made in converting the f - p' interaction to the f - p'' interaction. This second 0^+ state moves from 2.5 MeV in the f - p' spectrum to 4.5 MeV in the f - p'' spectrum. These values are, respectively, 1.0 MeV below and 1.0 above the observed 0^+ level at 3.52 MeV.

These results all suggest that in the effective Hamiltonian of Kuo and Brown, the interactions of $f_{7/2}$ particles with $p_{1/2}$ and $f_{5/2}$ particles are too strong. Note that if we had included in our calculation all second-order perturbations of the $p_{1/2}$ and $f_{5/2}$ single-particle strengths due to f - p -shell configurations, then the positions of these $p_{1/2}$ and $f_{5/2}$ strengths would have been even lower than in the f - p (KB) model.

V. GROUND-STATE BINDING ENERGIES AND WAVE GROUND-STATE FUNCTIONS

In the preceding sections we have discussed excitation energies within each isotope. In this section we discuss ground-state binding energies with respect to ^{40}Ca . In our calculations the binding energy of each $f_{7/2}$ neutron to the ^{40}Ca core is set equal to the observed ground-state binding en-

ergy of ^{41}Ca - i.e., we set the single-particle energy of the $f_{7/2}$ neutron at -8.36 MeV.¹⁴ The relative positions of the other single-particle energies are the same as those listed in Table I. In Table XII we show calculated and experimentally determined¹⁴ ground-state binding energies relative to ^{40}Ca . Table XII includes results from all the models of Figs. 10-18 except the $f_{7/2}$ -expt model. (We will discuss the column headed Talmi later.) The binding energy for ^{47}Ca in the f - p - g model is omitted because the calculation of the $J=\frac{7}{2}^-$ states in ^{47}Ca in that space is too large for our present capabilities.

From Table XII we see that for the models in which the published KB numbers were used, each ground-state binding energy increases as orbits are added (as must obviously happen). For $^{42-48}\text{Ca}$, the experimentally determined numbers are intermediate between the numbers calculated from the f - p model and the f - p - g model. This pattern is analogous to the pattern found for excitation energies. The inclusion of the $g_{9/2}$ orbit in the shell-model calculation leads to too much binding energy. Thus, a weakening of the effect of this orbit would give better agreement with experiment. If we use the f - p' model, we see that the agreement between calculation and experiment is significantly improved.

It is not clear how to assess the quality of agreement between theory and experiment here. For the f - p' model, the rms deviation of theory from experiment is 0.16 MeV for $^{42-48}\text{Ca}$. This might seem quite satisfactory agreement, since the total binding energy with respect to ^{40}Ca varies from 19.83 MeV in ^{42}Ca to 73.94 MeV in ^{48}Ca . However, a large part of this binding energy comes from the one-body part of the interaction. If we assume the ground states of $^{42-48}\text{Ca}$ are pure- $f_{7/2}^n$ states, then the one-body contribution is 16.72 MeV in ^{42}Ca , and 66.88 MeV in ^{48}Ca . Thus in terms of the *two-body* part of the effective interaction, the agreement is not as spectacular as

TABLE XII. Ground-state binding energies with respect to ^{40}Ca . The units are MeV. The binding energies under Talmi are results of the one-shell approximation of Talmi (see Ref. 35).

	Expt ^a	$\frac{7}{2}$	$\frac{7}{2}-\frac{3}{2}$	f - p (KB)	f - p - g	f - p'	Talmi
^{42}Ca	19.83	18.53	18.65	19.32	20.00	19.60	19.86
^{43}Ca	27.76	26.58	26.72	27.36	28.13	27.68	27.78
^{44}Ca	38.90	36.45	36.70	37.96	39.38	38.56	38.80
^{45}Ca	46.32	44.20	44.47	45.58	47.18	46.27	46.26
^{46}Ca	56.72	53.76	54.12	55.73	57.96	56.70	56.82
^{47}Ca	64.00	61.20	61.55	62.82	...	63.96	63.82
^{48}Ca	73.94	70.46	70.84	72.50	75.69	73.90	73.92
^{49}Ca	79.08	...	77.86	79.50	82.69	78.69	...
^{50}Ca	85.43	...	86.19	88.31	91.37	85.87	...

^aFrom Ref. 14.

it first appears. A simple calculation of these binding energies, by Talmi,³⁵ bears on the significance of these results. He has shown that if one assumes pure- $f_{7/2}^n$ states for the ground states of $^{42-48}\text{Ca}$, and if one uses an effective Hamiltonian of the usual one-body plus two-body form, then the total binding energy can be written as

$$B. E. (f_{7/2}^n) = nA + \frac{n(n-1)}{2}B + \begin{bmatrix} n \\ 2 \end{bmatrix} C, \quad (2)$$

where

$$\begin{bmatrix} n \\ 2 \end{bmatrix} = \begin{cases} \frac{1}{2}n & \text{for } n \text{ even,} \\ \frac{1}{2}(n-1) & \text{for } n \text{ odd.} \end{cases} \quad (3)$$

Here A is the one-body interaction energy of an $f_{7/2}$ particle with the ^{40}Ca core, while B and C are simple linear combinations of the matrix elements of the two-body part of the effective Hamiltonian. In (2), the second term is proportional to the number of two-body interactions in the n -particle system, and the third term introduces pairing effects. Talmi treated A , B , and C as parameters: He varied them so as to minimize the rms deviation between theory and experiment for the ground-state binding energies of $^{42-48}\text{Ca}$. The resulting theoretical binding energies are shown in Table XII under the heading Talmi. Their rms deviation for $^{42-48}\text{Ca}$ is 0.09 MeV. Thus we see that the binding energies can be calculated to a quite high degree of accuracy with a rather simple model.

In Table XIII, we show what percentage of each ground state is made up of the lowest-energy shell-model configuration; i.e., we show how much of each ground state for $^{42-48}\text{Ca}$ is pure $f_{7/2}^n$, how much of ^{49}Ca is $f_{7/2}^8 p_{3/2}$, and how much of ^{50}Ca is $f_{7/2}^8 p_{3/2}^2$. In the f - p model this dominant configuration decreases in intensity as the mass increases. In the f - p' model this intensity remains much more constant - at about 90%, up through ^{49}Ca . Within the accuracy of the spectroscopic factors deduced from experiment, this kind of con-

stant behavior is consistent with the empirically determined results on strengths for ground-state-to-ground-state transitions. (See Tables III-XI.)

VI. SUMMARY OF RESULTS

We have presented here the results of a series of calculations of the calcium isotopes from $A = 42$ to $A = 50$ in terms of the conventional shell model. We have assumed an inert ^{40}Ca core and allowed active $f_{7/2}$, $p_{3/2}$, $p_{1/2}$, and $f_{5/2}$ neutrons, and sometimes active $g_{9/2}$ neutrons. We believe that we have included all those configurations involving an inert ^{40}Ca core that are important in the structure of low-lying states of the calcium isotopes. In our first series of calculations, we used the shell-model interaction derived for the f - p -shell region from the Hamada-Johnston potential by Kuo and Brown.⁷ To specify the one-body part of the Hamiltonian, we used the same single-particle energies as were used by Kuo and Brown. When this Hamiltonian is used in our shell-model vector spaces that exclude two-particle excitations to the $g_{9/2}$ orbit, the calculated spectra are too compressed with respect to the observed spectra. But when such $g_{9/2}^2$ excitations are included, the calculated spectra become too expanded compared to experiment; i.e., when these $g_{9/2}^2$ excitations are explicitly included in the shell-model calculations, their effects are too strong. The results of these calculations suggest that: (1) In the Kuo-Brown interaction, the interaction of the $f_{7/2}$ particles with particles in the $p_{3/2}$, $p_{1/2}$, and $f_{5/2}$ orbits are too strong; and/or (2) because of imperfections in the Kuo-Brown effective interaction, it is advisable to modify it with an A -dependent term which will lead to an increase in the energy separation of the $f_{7/2}$ orbit from the other active orbits as the mass increases.

We next discussed a series of shell-model calculations in which no $g_{9/2}$ nucleons were allowed, and in which we used a modified version of the Kuo-Brown interaction. With this modified interaction, the observed energy levels of the $f_{7/2}$ states and of the strong $p_{3/2}$ single-particle states in ^{42}Ca - ^{49}Ca are quite well reproduced, as are measured binding energies of the ground states with respect to ^{40}Ca . The calculated spectroscopic factors for $f_{7/2}$ -neutron transfers between the various calcium isotopes are in good agreement with experiment. The observed centroids for the $p_{3/2}$ single-particle strengths are also reproduced reasonably well. It was difficult to reach any firm conclusions with regard to the $p_{1/2}$ and $f_{5/2}$ strengths, for two reasons: (1) There is very little firm experimental information on such strengths; and (2) our basis-vector space for

TABLE XIII. Percentage of ground-state wave function made up of pure- $(f_{7/2})^n$ configuration in ^{42}Ca to ^{50}Ca .

	f - p	f - p'
^{42}Ca	92	92
^{43}Ca	91	92
^{44}Ca	82	87
^{45}Ca	81	88
^{46}Ca	72	84
^{47}Ca	72	87
^{48}Ca	57	86
^{49}Ca	70 ($f_{7/2}^8, p_{3/2}$)	84 ($f_{7/2}^8, p_{3/2}$)
^{50}Ca	61 ($f_{7/2}^8, p_{3/2}^2$)	46 ($f_{7/2}^8, p_{3/2}^2$)

states with significant $p_{1/2}$ and $f_{5/2}$ strength is less complete than for states with strong $f_{7/2}$ and $p_{3/2}$ strengths. Within the basis-vector spaces we have used, and with the Hamiltonians we have used, there are no calculated levels that correspond with the observed second 0^+ and 2^+ states in ^{42}Ca , ^{44}Ca , and ^{46}Ca . This result suggests that these observed second 0^+ and 2^+ states contain large components based on configurations not included

in these calculations. In particular, we think that these second 0^+ and 2^+ states are predominantly core-excited.

ACKNOWLEDGMENT

We are indebted to T. T. S. Kuo for the use of his computer programs for calculating some of the effective interactions discussed here.

†Research sponsored by the U. S. Atomic Energy Commission under contract with Union Carbide Corporation.

*Present address: Michigan State University, East Lansing, Michigan.

¹I. Talmi and I. Unna, *Ann. Rev. Nucl. Sci.* **10**, 353 (1960).

²J. D. McCullen, B. Bayman, and L. Zamick, *Phys. Rev.* **134**, B515 (1964).

³J. N. Ginocchio and J. B. French, *Phys. Letters* **7**, 137 (1963).

⁴B. J. Raz and M. Soga, *Phys. Rev. Letters* **24**, 924 (1965).

⁵T. Engeland and E. Osnes, *Phys. Letters* **20**, 424 (1966).

⁶P. Federman and I. Talmi, *Phys. Letters* **22**, 469 (1966).

⁷T. T. S. Kuo and G. E. Brown, *Nucl. Phys.* **A114**, 241 (1968).

⁸E. C. Halbert, J. B. McGrory, B. H. Wildenthal, and S. P. Pandya, to be published.

⁹J. B. French, E. C. Halbert, J. B. McGrory, and S. S. M. Wong, in *Advances in Nuclear Physics*, edited by M. Baranger and E. Vogt (Plenum Publishing Corporation, New York, 1969), Vol. 3.

¹⁰T. T. S. Kuo and G. E. Brown, *Nucl. Phys.* **85**, 40 (1966).

¹¹T. T. S. Kuo, *Nucl. Phys.* **103**, 71 (1967).

¹²T. A. Belote, A. Sperduto, and W. E. Buechner, *Phys. Rev.* **139**, 80 (1965).

¹³K. K. Seth, J. Picard, and G. R. Satchler, to be published.

¹⁴*Nuclear Data Sheets*, compiled by K. Way *et al.* (Printing and Publishing Office, National Academy of Sciences - National Research Council, Washington, D. C.).

¹⁵W. J. Gerace and A. M. Green, *Nucl. Phys.* **A93**, 110 (1967).

¹⁶P. Federman, *Nucl. Phys.* **A124**, 363 (1969).

¹⁷B. H. Flowers and L. D. Skouras, *Nucl. Phys.* **A116**, 529 (1968).

¹⁸G. Sartoris and L. Zamick, *Phys. Rev.* **167**, 1035

(1968), and L. Zamick, private communication.

¹⁹To perform the least-squares searches we used computer programs developed for this purpose by P. W. M. Glaudemans and B. H. Wildenthal. The method is described by Glaudemans in *Nucl. Phys.* **56**, 529 (1964).

²⁰The next step would be to limit this kind of renormalization to correction of those Kuo-Brown matrix elements involving $f_{7/2}$ and/or $p_{3/2}$ particles only. Such a limitation would avoid the small denominators, and yet adjust those two-body matrix elements which are most important for the low-lying states of the calcium isotopes. It would adjust all the matrix elements that were changed in going from KB to KB' - and some others, too.

²¹E. P. Lippincott and A. M. Bernstein, *Phys. Rev.* **163**, 1170 (1967).

²²J. L. Yntema, to be published.

²³J. H. Bjerregaard, O. Hansen, O. Nathan, R. Chapman, S. Hinds, and R. Middleton, *Nucl. Phys.* **A103**, 33 (1967).

²⁴W. E. Dorenbusch, T. A. Belote, and O. Hansen, *Phys. Rev.* **146**, 734 (1966).

²⁵C. Glashauser and J. Thirion, in *Advances in Nuclear Physics*, edited by M. Baranger and E. Vogt (Plenum Publishing Corporation, New York, 1969), Vol. 2.

²⁶J. H. Bjerregaard and O. Hansen, *Phys. Rev.* **155**, 1229 (1967).

²⁷J. B. McGrory and B. H. Wildenthal, *Phys. Letters* **28**, 237 (1968).

²⁸P. W. M. Glaudemans, B. H. Wildenthal, and J. B. McGrory, *Phys. Letters* **21**, 427 (1966).

²⁹S. Cohen, R. D. Lawson, and S. P. Pandya, *Nucl. Phys.* **A114**, 541 (1968).

³⁰J. Rapaport, W. E. Dorenbusch, and T. A. Belote, *Phys. Rev.* **156**, 1255 (1967).

³¹J. H. Bjerregaard, O. Hansen, and G. Sidenius, *Phys. Rev.* **138**, B1097 (1965).

³²R. J. Peterson, *Phys. Rev.* **170**, 1003 (1968).

³³K. Kolltveit, *Nucl. Phys.* **A126**, 115 (1969).

³⁴E. Kashy, A. Sperduto, H. A. Enge, and W. W. Buechner, *Phys. Rev.* **135**, 865 (1964).

³⁵I. Talmi, *Phys. Rev.* **107**, 326 (1957).